Published by Institute of Physics Publishing for SISSA

Received: *December 4, 2006*
Revised: *January 31, 2007*
Accepted: *February 15, 2007*
Published: *March 19, 2007*

Logarithmic electroweak corrections to $e^+e^- \to \nu_e\bar{\nu}_e W^+W^-$

Elena Accomando

Dipartimento di Fisica Teorica, Università di Torino, and INFN, Sezione di Torino, Via P. Giuria 1, 10125 Torino, Italy
E-mail: accomand@to.infn.it

Ansgar Denner

Paul Scherrer Institut, Würenlingen und Villigen CH-5232 Villigen PSI, Switzerland
E-mail: Ansgar.Denner@psi.ch

Stefano Pozzorini

Max-Planck-Institut für Physik (Werner-Heisenberg-Institut) Föhringer Ring 6, D-80805 München, Germany
E-mail: pozzorin@particle.uni-karlsruhe.de

Abstract: We consider W-boson scattering at high-energy e^+e^- colliders and study one-loop logarithmic electroweak corrections within the Standard Model assuming a light Higgs boson. We present explicit analytical results for $W^+W^- \to W^+W^-$. Using the equivalent vector-boson approximation, we have implemented these corrections into a Monte Carlo program for the process $e^+e^- \to \nu_e\bar{\nu}_e W^+W^-$. The quality of the equivalent vector-boson approximation and of the logarithmic high-energy approximation for the electroweak corrections is discussed in detail. The impact of the radiative effects is quantitatively analysed. The corrections are negative and their size, typically of the order of 10%, increases with energy reaching up to −20% and −50% at the ILC and CLIC, respectively.

Keywords: Spontaneous Symmetry Breaking, Standard Model.

JHEP03(2007)078

© SISSA 2007

Contents

1. Introduction **1**

2. Process definition and numerical setup **3**

3. Strategy of the calculation **5**
- 3.1 Equivalent vector-boson approximation 6
- 3.2 Virtual electroweak corrections 10

4. Numerical results **13**

5. Conclusions **18**

A. On-shell projection **19**

B. Logarithmic electroweak corrections **19**
- B.1 Structure of the one-loop logarithmic corrections 21
- B.2 Leading soft-collinear corrections 22
- B.3 Subleading soft-collinear corrections 23
- B.4 Single logarithms from collinear singularities 27
- B.5 Single logarithms from parameter renormalization 27

C. Longitudinal gauge bosons **28**

D. Born matrix elements in the high-energy limit **31**

E. Electromagnetic virtual and real contributions **34**

JHEP03(2007)078

1. Introduction

One of the foremost open questions in particle physics concerns the mechanism of electroweak symmetry breaking. Depending on its realization in nature, the understanding of this subtle mechanism must be approached in different ways. If the Standard Model (SM) with a light Higgs boson is realized, the Higgs boson can be directly produced and its properties investigated. If the Higgs boson is heavy or absent, a complementary approach must be pursuit. In this case, information can be extracted from the scattering of longitudinally polarized gauge bosons. In fact, at high energies, longitudinal vector bosons unveil their origin as Goldstone bosons and, by virtue of the equivalence theorem, reflect the dynamics of electroweak symmetry breaking.

Accordingly, vector-boson scattering (VBS) looks very much different in these different scenarios of electroweak symmetry breaking. In the SM with a light Higgs boson the gauge sector remains weakly interacting and the cross section can be reliably predicted within perturbation theory. In the alternative scenario, where a light Higgs boson is absent, perturbative unitarity is violated, and the longitudinal gauge bosons must become strongly interacting at high energies thus allowing for non-perturbative restoration of unitarity [1].

In the past years, a variety of models have been proposed to parametrize the strongly-interacting electroweak gauge sector, and to recover unitarity (see for instance ref. [2] and references therein). The common prediction is an enhanced production of longitudinal gauge bosons. However, the phenomenological consequences as well as the new particles the various models provide can be sensibly different. They can be classified into two main groups [3]. In the most optimistic case, one could expect many new resonances at future colliders. In the less favorable scenario, the mass of any new particle could be much bigger than the energy scale probed at the planned accelerators. In this case, the indirect effect of such particles would only consist in a slight increase of the VBS event rate at high energy compared to the predictions of the SM with a light Higgs boson.

Several studies have been performed in order to estimate the possible reach of the future lepton and hadron colliders [2 – 8]. The answers strongly depend on energy and luminosity parameters. Also a good control of the SM background can prove essential, particularly for the less favorable case.

In this paper, we consider VBS within the SM at the planned e^+e^- colliders. For the International Linear Collider (ILC) [9] we consider a centre-of-mass (CM) energy $\sqrt{s} = 1\,\text{TeV}$ and for the Compact Linear Collider (CLIC) [10] $\sqrt{s} = 3\,\text{TeV}$. More precisely, we focus on the production of W-boson pairs plus neutrinos in the reaction $e^+e^- \to \nu_e\bar{\nu}_e W^+W^-$. For the projected luminosity $L = 1\,\text{ab}^{-1}$, the experimental collaborations will collect thousands of events coming from VBS in the high-energy domain, where a possible strongly-interacting regime of the weak gauge sector could manifest itself.

To match the envisaged statistical precision, the SM predictions have to be computed beyond lowest order. Indeed, in the very same high-energy region of interest, the electroweak radiative effects are enhanced by electroweak Sudakov logarithms [11 – 15], i.e. double and single logarithms of the ratio of the scattering energy over the vector-boson mass (recent progress in the evaluation of electroweak Sudakov logarithms is discussed in ref. [16]). At $\mathcal{O}(\alpha)$, these corrections can reach several tens of per cent, as confirmed by various analyses performed for different processes at lepton and hadron colliders [17 – 26]. Hence, in the case at hand, they have to be taken into account in order to search for small deviations between data and SM predictions that might appear as a signal of strongly interacting electroweak symmetry breaking.

So far, the process $e^+e^- \to \nu_e\bar{\nu}_e W^+W^-$ has been computed at Born level, and found promising for investigating electroweak symmetry breaking at high invariant masses of the produced W-boson pairs [7, 27, 28]. The aim of our work is to study the contributions of the electroweak Sudakov logarithms, which represent the dominant electroweak corrections at high energies.

Our calculation is performed within the SM assuming a light Higgs boson. Strongly

JHEP03(2007)078

interacting vector bosons are not expected in this scenario. Nevertheless, also if a light Higgs boson is found at the LHC, the WW plus missing energy final state will be investigated in detail at linear colliders, looking for anomalous effects or new resonances. For the more interesting case where no light Higgs boson is present our calculation is not directly applicable. However, the logarithmic Sudakov enhancement discussed in this paper is not due to the Higgs boson and depends only weakly (at the subleading-logarithmic level) on the Higgs-boson mass. This radiative effect originates from soft-collinear gauge bosons and will be present also in the no-Higgs scenario.

For the calculation of the electroweak corrections we use the equivalent vector-boson approximation following the approach of ref. [29]. Within this approximation we only consider virtual $\mathcal{O}(\alpha)$ corrections to the WW-scattering subprocess. These corrections are calculated using the method of refs. [12, 13] in the high-energy logarithmic approximation. As in refs. [12, 13], the virtual photonic corrections are split into a symmetric-electroweak and a purely electromagnetic part, which originate from above and below the electroweak scale, respectively. The former part is in practice obtained by setting the photon mass equal to M_{W} in the photonic virtual corrections, and is infrared finite. The infrared singularities are contained in the purely-electromagnetic part and are cancelled when including soft-photon bremsstrahlung. Both the symmetric-electroweak and purely-electromagnetic parts are included in our analytical results. However the latter is omitted in our numerical studies since it strictly depends on the experimental setup.

The paper is organized as follows. In section 2 we define the process and give the setup for the numerical evaluation. In section 3 we describe the strategy of the calculation and discuss the quality of the used approximations. Numerical results are presented in section 4, and section 5 contains the summary. Explicit analytical results are listed in the appendices.

2. Process definition and numerical setup

We consider the production of a W-boson pair plus two neutrinos in electron-positron collisions:

$$\mathrm{e}^+\mathrm{e}^- \to \nu_\mathrm{e}\bar{\nu}_\mathrm{e}\mathrm{W}^+\mathrm{W}^-. \tag{2.1}$$

This process contains the VBS subprocess $\mathrm{W}^+\mathrm{W}^- \to \mathrm{W}^+\mathrm{W}^-$ generically described by the first Feynman diagram in figure 1. The WW-scattering signal is not the only contribution to the final state in (2.1). The irreducible background, exemplified by the second and third Feynman graphs in figure 1, is indeed sizeable and must be properly suppressed in order to enhance the VBS signal-to-background ratio. A set of appropriate kinematical cuts to be imposed is summarized below.

In our analyses, we use the input values [30]

$$\begin{aligned} M_{\mathrm{W}} &= 80.403\,\mathrm{GeV}, & M_{\mathrm{Z}} &= 91.1876\,\mathrm{GeV}, \\ M_{\mathrm{H}} &= 120\,\mathrm{GeV}, & m_{\mathrm{t}} &= 174.2\,\mathrm{GeV}, \end{aligned} \tag{2.2}$$

JHEP03(2007)078

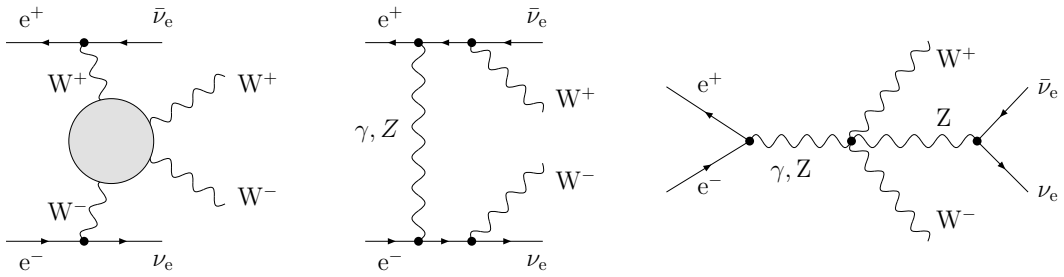

Figure 1: Feynman diagrams contributing to the process $e^+e^- \to \nu_e\bar{\nu}_e W^+W^-$. The first graph on the left is a generic representation of the WW-scattering signal. The remaining two diagrams are examples of irreducible background.

for vector-boson, Higgs-boson, and top-quark masses. All other fermions are taken to be massless. The sine s_W and cosine c_W of the weak mixing angle are fixed by

$$c_W^2 = 1 - s_W^2 = \frac{M_W^2}{M_Z^2}. \tag{2.3}$$

Moreover, we adopt the so called G_μ-scheme, which effectively includes higher-order contributions associated with the running of the electromagnetic coupling and the leading universal two-loop m_t-dependent corrections in the definition of α. Using

$$G_\mu = 1.16637 \times 10^{-5}\,\mathrm{GeV}^{-2}, \tag{2.4}$$

we have

$$\alpha = \sqrt{2} G_\mu M_W^2 s_W^2/\pi = 1/132.38\ldots. \tag{2.5}$$

In the following sections, we present results for a CM energy $\sqrt{s} = 1\,\mathrm{TeV}$, which can be reached at the ILC, and for $\sqrt{s} = 3\,\mathrm{TeV}$ as is planned for CLIC. In both cases we assume an integrated luminosity $L = 1\,\mathrm{ab}^{-1}$.

Based on the study of ref. [7], we have implemented a general set of cuts, proper for ILC and CLIC analyses, defined as follows. In the listed cuts, the numbers outside parentheses are used for $\sqrt{s} = 1\,\mathrm{TeV}$, those within parentheses for $\sqrt{s} = 3\,\mathrm{TeV}$.

- We require a W-boson transverse momentum $P_T(W^\pm) \geq 100(200)\,\mathrm{GeV}$, since the production of longitudinal vector bosons, i.e. the VBS signal, is enhanced for large scattering angles and high energies. Moreover, this cut removes events dominated by t-channel photon exchange in subprocesses.

- We require $|\cos\theta(W^\pm)| \leq 0.8$, where $\theta(W^\pm)$ is the angle of the produced $W^\pm$ boson with respect to the incoming positron in the laboratory frame, since the VBS signal is characterized by central W-boson production. This cut also removes events dominated by t-channel photon exchange in subprocesses.

JHEP03(2007)078

- We require $|y(\mathrm{W}^+) - y(\mathrm{W}^-)| \leq 2$, where $y(\mathrm{W}^\pm)$ is the rapidity of the produced $\mathrm{W}^\pm$ boson defined as $y = 0.5 \ln[(E+P_\mathrm{L})/(E-P_\mathrm{L})]$ and E and P_L are the W-boson energy and component of the momentum along the beam axis, respectively. This additional angular cut ensures the production of central W bosons also in the CM frame of vector-boson scattering.

- We require a transverse momentum of the W-boson pair $P_\mathrm{T}(\mathrm{WW}) \geq 40(50)\,\mathrm{GeV}$. This cut suppresses the reducible background coming from the process $\mathrm{e}^+\mathrm{e}^- \to \mathrm{e}^+\mathrm{e}^-\mathrm{W}^+\mathrm{W}^-$, i.e. $\gamma\gamma$ fusion, when the two produced $\mathrm{e}^\pm$ are emitted forward/backward.

- We require a neutrino-pair invariant mass $M(\nu_\mathrm{e}\bar{\nu}_\mathrm{e}) \geq 150(200)\,\mathrm{GeV}$. This cut removes $\mathrm{W}^+\mathrm{W}^-\mathrm{Z}$ production events, in which the neutrinos come from the Z-boson decay (see the last graph in figure 1).

- We require a diboson invariant mass $M(\mathrm{WW}) \geq 400(700)\,\mathrm{GeV}$. Selecting high diboson CM energies allows one to test a possible strongly-interacting regime of the electroweak gauge sector.

3. Strategy of the calculation

In this section, we describe the main ingredients of our calculation. We summarize the adopted approximations and discuss their domain of applicability.

We consider the process (2.1), with two on-shell W bosons and two neutrinos in the final state. For this process, exact lowest-order matrix elements are employed in our Monte Carlo, simultaneously accounting for signal and irreducible background. We moreover use the complete four-particle phase space and exact kinematics.

Computing $\mathcal{O}(\alpha)$ electroweak corrections in leading-pole approximation, as in refs. [31 – 33] and references therein, has revealed successful for analysing WW physics at LEP2. A similar philosophy can be adopted for the incoming bosons in VBS at energies that are large compared to the gauge-boson masses, since this process is dominated by small invariant masses of these incoming bosons, which are thus relatively close to their mass shell, even though these invariant masses are actually negative.

We thus compute the $\mathcal{O}(\alpha)$ electroweak corrections to the process (2.1) in equivalent-vector-boson approximation (EVBA). As discussed in the introduction, we do not include real photonic corrections. For the virtual corrections we work in the logarithmic approximation and we restrict our calculation to the infrared-finite part coming from above the electroweak scale. These corrections correspond to the case where the photon has effectively the mass M_W and are precisely defined in ref. [12]. This approach is sensible since at high energies, the electroweak corrections are dominated by double and single logarithms of the ratio of the energy to the electroweak scale. Hence, keeping only the terms proportional to $\alpha \log^2(\hat{s}/M_\mathrm{W}^2)$ and $\alpha \log(\hat{s}/M_\mathrm{W}^2)$, where $\hat{s}$ is the CM energy of the VBS subprocess, provides the bulk of the radiative corrections.

JHEP03(2007)078

3.1 Equivalent vector-boson approximation

In EVBA, the process $e^+e^- \to \nu_e\bar{\nu}_e W^+W^-$ is entirely described by the subset of Feynman diagrams generically represented by the first graph in figure 1. The approximation considers in fact only those contributions to the final state that come from the scattering of the two vector bosons emitted by the incoming particles. The goodness of the approximation thus relies on the assumption that such contributions are indeed the dominating ones in the considered kinematical domain. This hypothesis depends on the process at hand, and can only be checked against an exact computation. In this section, we discuss the reliability of the EVBA in describing the process $e^+e^- \to \nu_e\bar{\nu}_e W^+W^-$ and its validity domain.

In implementing the EVBA, we follow the approach of ref. [29]. This method preserves the exact kinematics of the process, a very useful property for imposing realistic cuts.

We assign the following set of momenta p_i and helicities $\lambda_i = 0, \pm 1$ to the particles involved in the process we are considering:

$$e^+(p_1,+)\, e^-(p_2,-) \to \nu_e(p_3,-)\, \bar{\nu}_e(p_4,+)\, W^+(p_5,\lambda_5)\, W^-(p_6,\lambda_6). \tag{3.1}$$

In EVBA only left-handed lepton chiralities are relevant, since the electrons and neutrinos couple always to W bosons.[1] Using the unitary gauge and writing the propagators of the two incoming W bosons, emitted by the initial $e^\pm$ and exchanged in t channel (see figure 1), as a sum over the vector-boson polarizations

$$\frac{1}{p^2 - M_W^2}\left(-g^{\mu\nu} + \frac{p^\mu p^\nu}{M_W^2}\right) = \sum_{\lambda=-1,0,1} \frac{\epsilon_\lambda^\mu(p)\epsilon_\lambda^{*\nu}(p)}{p^2 - M_W^2}, \tag{3.2}$$

the exact amplitude corresponding to the first graph in figure 1 assumes the form

$$\begin{aligned}\mathcal{M}^{e^+e^-\to\nu_e\bar{\nu}_e W^+W^-}(p_1,p_2,p_3,p_4,p_5,p_6;\lambda_5,\lambda_6) &= \frac{1}{q_+^2 - M_W^2}\,\frac{1}{q_-^2 - M_W^2} \\ &\times \sum_{\lambda_+,\lambda_-=-1,0,1} \mathcal{M}^{e^+\to\bar{\nu}_e W^+}(p_1,p_4,q_+;\lambda_+)\, \mathcal{M}^{e^-\to\nu_e W^-}(p_2,p_3,q_-;\lambda_-) \\ &\times \mathcal{M}^{W^+W^-\to W^+W^-}(q_+,q_-,p_5,p_6;\lambda_+,\lambda_-,\lambda_5,\lambda_6).\end{aligned} \tag{3.3}$$

In EVBA the off-shell amplitude for WW scattering, $\mathcal{M}^{W^+W^-\to W^+W^-}$, is replaced by a suitably defined on-shell amplitude. In this way gauge invariance of this amplitude is ensured, and artifacts from using an incomplete off-shell amplitude are avoided. Modifications of the on-shell amplitude are necessary in order to describe the dependence of the off-shell amplitude on the off-shell masses $q_\pm^2$ to a satisfactory accuracy. We here follow the approach of ref. [29] which describes the extrapolation to off-shell masses by simple proportionality factors for each incoming vector boson. These are chosen to be equal to 1 for transverse bosons. For each longitudinal W^+ or W^- boson, the on-shell amplitude is multiplied by a factor $M_W/\sqrt{-q_\pm^2}$ in order to describe the singular behaviour $\epsilon_{\lambda=0}^\mu(q_\pm) \sim 1/\sqrt{-q_\pm^2}$ of the

[1] Instead, the exact matrix elements that we employ for our tree-level predictions receive (background) contributions also from right-handed leptons.

JHEP03(2007)078

$\sigma_{\rm Born}(e^+e^- \to \nu_e\bar{\nu}_e W^+W^-)$			
$\sqrt{s}$ [TeV]	$\sigma_{\rm exact}$ [fb]	$\sigma_{\rm EVBA}$ [fb]	$\Delta_{\rm EVBA}$ [%]
1	0.595	0.479	19.5
3	3.507	3.471	1.0

Table 1: Exact lowest-order cross section (second column) as well as total cross section in EVBA (third column) and their difference in per cent of the exact result (fourth column). Kinematical cuts as in section 2 are applied.

off-shell longitudinal polarization vectors. One can thus write

$$\begin{aligned}\mathcal{M}^{e^+e^-\to\nu_e\bar{\nu}_e W^+W^-}_{\rm EVBA}(p_1,p_2,p_3,p_4,p_5,p_6;\lambda_5,\lambda_6) &= \frac{1}{q_+^2-M_W^2}\,\frac{1}{q_-^2-M_W^2}\\ &\times\sum_{\lambda_+,\lambda_-=-1,0,1}\mathcal{M}^{e^+\to\bar{\nu}_e W^+}(p_1,p_4,q_+;\lambda_+)\,\mathcal{M}^{e^-\to\nu_e W^-}(p_2,p_3,q_-;\lambda_-)\\ &\times\mathcal{M}^{W^+W^-\to W^+W^-}(q_+^{\rm on},q_-^{\rm on},p_5,p_6;\lambda_+,\lambda_-,\lambda_5,\lambda_6)\\ &\times\left[\frac{M_W}{\sqrt{-q_+^2}}\,\delta_{\lambda_+,0}+\delta_{\lambda_+,\pm}\right]\left[\frac{M_W}{\sqrt{-q_-^2}}\,\delta_{\lambda_-,0}+\delta_{\lambda_-,\pm}\right],\end{aligned}\tag{3.4}$$

where $q_\pm^{\rm on}$ are the on-shell projected momenta of the two incoming W bosons. The definition of the on-shell projection is given in appendix A. Note that the W-boson momenta in the matrix elements $\mathcal{M}^{e^+\to\bar{\nu}_e W^+}$ and $\mathcal{M}^{e^-\to\nu_e W^-}$ are not projected on shell.

In order to proceed, in ref. [29] the squared amplitude was considered and the contributions of the matrix elements $\mathcal{M}^{e^+\to\bar{\nu}_e W^+}$ and $\mathcal{M}^{e^-\to\nu_e W^-}$ were transformed into vector-boson luminosities. Instead, we work at the matrix element level and compute the three amplitudes on the right-hand side of (3.4) with the help of `PHACT` [34], a routine based on the helicity-amplitude method of ref. [35].

In table 1, we show the comparison between the EVBA and the exact lowest-order result for the total cross section. We select the kinematical domain where we expect new-physics effects related to strongly interacting vector bosons to be enhanced. Such a region, characterized by high diboson invariant masses and large scattering angles of the two produced W bosons, is selected via appropriate cuts described in detail in section 2. At $\sqrt{s} = 1\,\text{TeV}$ and $\sqrt{s} = 3\,\text{TeV}$ the accuracy of the EVBA for the total cross section, $\Delta_{\rm EVBA} = (\sigma_{\rm exact} - \sigma_{\rm EVBA})/\sigma_{\rm exact}$, amounts to about 20% and 1%, respectively.

The integrated cross section gives only a partial information on the goodness of the EVBA. In order to display more extensively the reliability of this approximation in the selected kinematical domain, in figures 2 and 3 we analyse distributions in both energy-like and angular-like variables. In particular, we consider four observables of interest:

- diboson invariant mass $M(\text{WW})$,
- diboson transverse momentum $P_{\rm T}(\text{WW})$,

JHEP03(2007)078

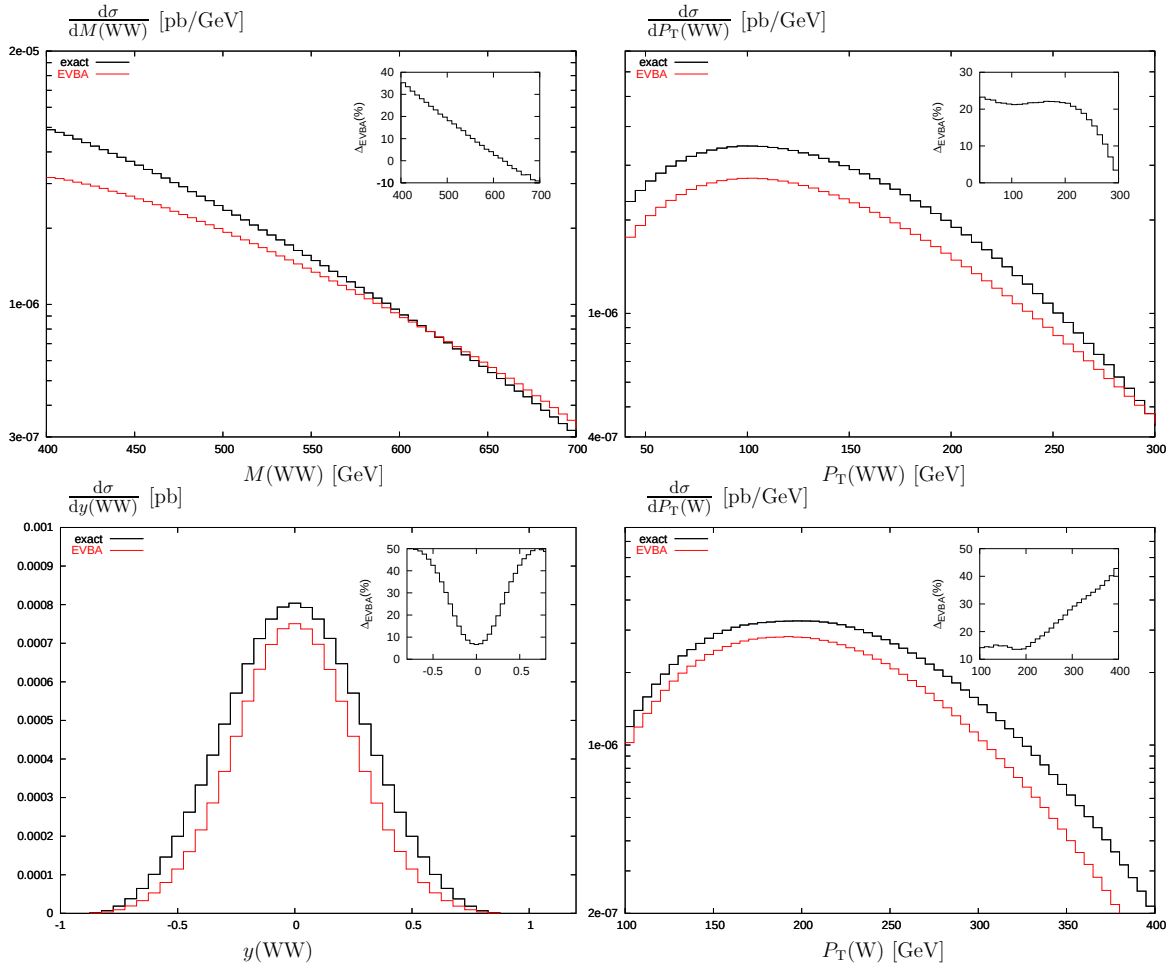

Figure 2: Lowest-order distributions for $\sqrt{s} = 1\,\text{TeV}$ from the exact matrix elements and in EVBA: invariant mass of the diboson pair (upper left), transverse momentum of the diboson pair (upper right), rapidity of the diboson pair (lower left), transverse momentum of the produced W boson (lower right). The inset plots show the relative difference Δ_{EVBA} in per cent. Standard cuts are applied.

- diboson rapidity $y(\text{WW}) = 0.5 \ln \left[\frac{E(\text{WW}) + P_{\text{L}}(\text{WW})}{E(\text{WW}) - P_{\text{L}}(\text{WW})} \right]$,
- W-boson transverse momentum $P_{\text{T}}(\text{W}) = P_{\text{T}}(\text{W}^+)$.

The distributions in $P_{\text{T}}(\text{W}^-)$ and $P_{\text{T}}(\text{W}^+)$ are identical. We plot the lowest-order results of the EVBA and of the exact calculation for the two collider energies $\sqrt{s} = 1\,\text{TeV}$ and $\sqrt{s} = 3\,\text{TeV}$ in figure 2 and figure 3, respectively. The inset plots show the difference in per cent between the two results, i.e. $\Delta_{\text{EVBA}} = (\text{d}\sigma_{\text{exact}} - \text{d}\sigma_{\text{EVBA}})/\text{d}\sigma_{\text{exact}}$. For ILC and CLIC, in most of the regions that are not statistically irrelevant, the difference is below 25% and 20%, respectively. The increase for small $M(\text{WW})$ is not problematic, since the radiative corrections are small in this region (see section 4). As a remark, let us add that the agreement between EVBA and exact result reached in this analysis should not be taken as the best one can do. The quality of the approximation is sensibly cut-dependent. In this

JHEP03(2007)078

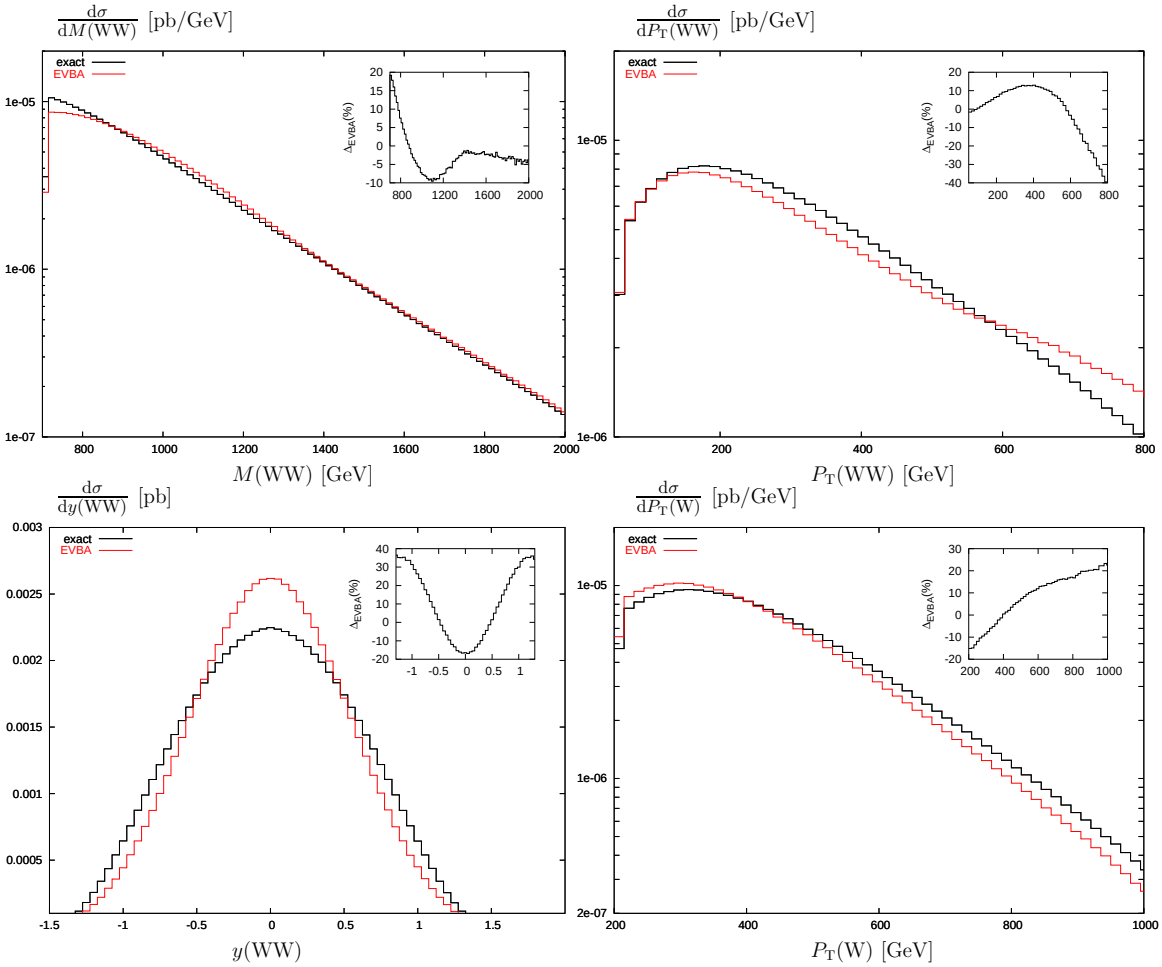

Figure 3: Lowest-order distributions for $\sqrt{s} = 3$ TeV from the exact matrix elements and in EVBA. Same conventions as in figure 2.

paper, following ref. [7] we have adopted generic cuts and, in principle, the EVBA could be improved imposing more stringent constraints. The choice of the set-up depends, however, on the particular analysis to be performed.

In the following, we use the EVBA for computing the $\mathcal{O}(\alpha)$ electroweak corrections, i.e. we consider only the corrections to the WW-scattering signal (first graph in figure 1) and neglect the corrections to the irreducible background. The lowest-order results are calculated using exact matrix elements, which include the contributions of signal and background. To estimate the $\mathcal{O}(\alpha)$ inaccuracy associated with the EVBA we assume that the corrections to the signal and the background behave similarly, i.e. that they are both enhanced by Sudakov effects. In this case the corrections to the background are expected to be of the order of the product of the corrections to the signal times the relative contribution of the background, i.e. the inaccuracy of the EVBA, at tree level. Since the corrections to the signal typically amount to 10–30%, the tree-level inaccuracy of the EVBA translates into a few-percent error for the full result. As shown in section 4, apart for the case of very

JHEP03(2007)078

high $P_{\mathrm{T}}(\mathrm{WW})$, the $\mathcal{O}(\alpha)$ uncertainty associated with the EVBA is always smaller than the expected statistical error at the ILC and CLIC.

3.2 Virtual electroweak corrections

In analogy with the leading-pole approximation for virtual corrections, the EVBA allows two types of radiative contributions, factorizable and non-factorizable ones. The former are those that can be associated to either the emission of one of the two incoming W bosons from the beam particles or the VBS subprocess. The latter are those connecting these subprocesses.

The non-factorizable corrections in leading-pole approximation consist only of photonic contributions. These corrections have been evaluated for W-boson pair production in $\mathrm{e}^+\mathrm{e}^-$ annihilation in refs. [36, 37]. There it was found that all infrared and mass-singular logarithms cancel between virtual and real corrections and that the remaining effects are small. In EVBA non-factorizable corrections do not only result from photon exchange between the subprocesses of W-boson-production and WW scattering but also from analogous exchanges of massive gauge bosons. These contributions deserve further investigations. In this paper, we do not consider the non-factorizable corrections but restrict ourselves to the calculation of the factorizable contributions.

The virtual factorizable corrections are represented by the schematic diagram of figure 4, in which the big blobs contain all one-loop corrections to the incoming W-boson-production and on-shell WW-scattering subprocesses. The corresponding matrix element can be written as

$$\begin{aligned}
\delta\mathcal{M}_{\mathrm{virt,EVBA,fact}}^{\mathrm{e}^+\mathrm{e}^-\to\nu_\mathrm{e}\bar{\nu}_\mathrm{e}\mathrm{W}^+_{\lambda_5}\mathrm{W}^-_{\lambda_6}} = {} & \frac{1}{q_+^2 - M_\mathrm{W}^2}\,\frac{1}{q_-^2 - M_\mathrm{W}^2} \\
& \times \sum_{\lambda_+,\lambda_-} \Big\{ \delta\mathcal{M}_{\mathrm{virt}}^{\mathrm{e}^+\to\bar{\nu}_\mathrm{e}\mathrm{W}^+_{\lambda_+}}\, \mathcal{M}_{\mathrm{Born}}^{\mathrm{e}^-\to\nu_\mathrm{e}\mathrm{W}^-_{\lambda_-}}\, \mathcal{M}_{\mathrm{Born,on}}^{\mathrm{W}^+_{\lambda_+}\mathrm{W}^-_{\lambda_-}\to\mathrm{W}^+_{\lambda_5}\mathrm{W}^-_{\lambda_6}} \\
& + \mathcal{M}_{\mathrm{Born}}^{\mathrm{e}^+\to\bar{\nu}_\mathrm{e}\mathrm{W}^+_{\lambda_+}}\, \delta\mathcal{M}_{\mathrm{virt}}^{\mathrm{e}^-\to\nu_\mathrm{e}\mathrm{W}^-_{\lambda_-}}\, \mathcal{M}_{\mathrm{Born,on}}^{\mathrm{W}^+_{\lambda_+}\mathrm{W}^-_{\lambda_-}\to\mathrm{W}^+_{\lambda_5}\mathrm{W}^-_{\lambda_6}} \\
& + \mathcal{M}_{\mathrm{Born}}^{\mathrm{e}^+\to\bar{\nu}_\mathrm{e}\mathrm{W}^+_{\lambda_+}}\, \mathcal{M}_{\mathrm{Born}}^{\mathrm{e}^-\to\nu_\mathrm{e}\mathrm{W}^-_{\lambda_-}}\, \delta\mathcal{M}_{\mathrm{virt,on}}^{\mathrm{W}^+_{\lambda_+}\mathrm{W}^-_{\lambda_-}\to\mathrm{W}^+_{\lambda_5}\mathrm{W}^-_{\lambda_6}} \Big\} \\
& \times \left[\frac{M_\mathrm{W}}{\sqrt{-q_+^2}}\,\delta_{\lambda_+,0} + \delta_{\lambda_+,\pm}\right] \left[\frac{M_\mathrm{W}}{\sqrt{-q_-^2}}\,\delta_{\lambda_-,0} + \delta_{\lambda_-,\pm}\right], \qquad (3.5)
\end{aligned}$$

where $\delta\mathcal{M}_{\mathrm{virt}}^{\mathrm{e}^+\to\bar{\nu}_\mathrm{e}\mathrm{W}^+_{\lambda_+}}$, $\delta\mathcal{M}_{\mathrm{virt}}^{\mathrm{e}^-\to\nu_\mathrm{e}\mathrm{W}^-_{\lambda_-}}$, and $\delta\mathcal{M}_{\mathrm{virt,on}}^{\mathrm{W}^+_{\lambda_+}\mathrm{W}^-_{\lambda_-}\to\mathrm{W}^+_{\lambda_5}\mathrm{W}^-_{\lambda_6}}$ denote the virtual corrections to the matrix elements for the W-boson-production and on-shell WW-scattering subprocesses. The index 'on' indicates that on-shell vector-boson momenta are used to calculate these matrix elements.

We calculate the factorizable $\mathcal{O}(\alpha)$ virtual corrections in logarithmic high-energy approximation including single and double enhanced logarithms, i.e. contributions proportional to $\alpha\log^2(\hat{s}/M_\mathrm{W}^2)$ and $\alpha\log(\hat{s}/M_\mathrm{W}^2)$, where $\hat{s}$ is the CM energy of the scattering subprocess. The logarithmic approximation yields the dominant corrections as long as CM

JHEP03(2007)078

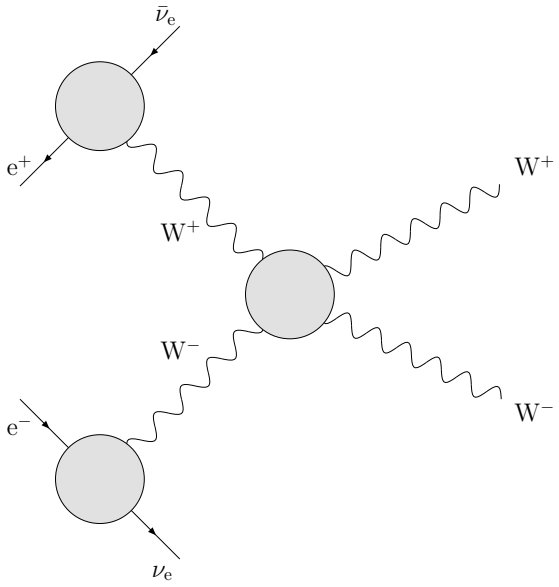

Figure 4: Structure of the virtual factorizable corrections in EVBA with one-loop contributions in the blobs.

energies and scattering angles are large. Pure angular-dependent logarithms of the form $\alpha \log^2(\hat{s}/\hat{r})$ and $\alpha \log(\hat{s}/\hat{r})$, with $\hat{r}$ equal to the Mandelstam variables $\hat{t}$ and $\hat{u}$ of the WW-scattering subprocess, are not included. However, angular-dependent terms of the form $\alpha \log(\hat{s}/\hat{r}) \log(\hat{s}/M_W^2)$ are taken into account. The validity of the results relies therefore on the assumption that all invariants are large compared with M_W^2 and approximately of the same size

$$\hat{s} \sim |\hat{t}| \sim |\hat{u}| \gg M_W^2. \tag{3.6}$$

This implies that the produced gauge bosons should be energetic and emitted at sufficiently large angles with respect to the beam. This is precisely the kinematical region where effects due to a possible strongly interacting regime of the gauge sector are maximally enhanced. In this region, the accuracy of the logarithmic high-energy approximation is expected to be of the order of a few per cent. We can thus reasonably adopt this approximation at e^+e^- colliders with energy in the 1–3 TeV range, where the experimental error is at the few-per-cent level. Since the emission subprocesses of the two incoming W bosons involve no large energy variable (they peak at $|q_\pm^2| \sim M_W^2$), the corresponding virtual corrections vanish in the logarithmic approximation. As a consequence, we do not consider the first two contributions on the right-hand side of (3.5) in the following. Moreover, for the $W^+W^- \to W^+W^-$ subprocess we take into account only the corrections to the dominating channels involving four transverse (TTTT) or two transverse and two longitudinal (LLTT, LTLT, TLTL) gauge bosons. The contributions of the channels with an odd number of

JHEP03(2007)078

$\sigma_{\rm Born}(e^+e^- \to \nu_e\bar{\nu}_e W^+_\lambda W^-_{\lambda'})$					
$\sqrt{s}$ [TeV]	$\sigma^{\rm TT}$ [fb]	$\sigma^{\rm TL}$ [fb]	$\sigma^{\rm LT}$ [fb]	$\sigma^{\rm LL}$ [fb]	$\sigma^{\rm tot}$ [fb]
1	0.500	0.0410	0.0410	0.0134	0.595
3	3.111	0.1786	0.1786	0.0390	3.507

Table 2: Born cross section for the process $e^+e^- \to \nu_e\bar{\nu}_e W^+_\lambda W^-_{\lambda'}$ and various polarizations ($\lambda, \lambda' = T, L$) of the produced W bosons. Kinematical cuts as specified in section 2 are applied.

longitudinally polarized W bosons are suppressed by $M_W/\sqrt{\hat{s}}$, and those of the channels LTTL and TLLT by $M_W^2/\hat{s}$. Moreover, the configurations with two final-state longitudinal W bosons are numerically small within the SM with a light Higgs boson. As shown in table 2, for $M_H = 120\,\text{GeV}$, the cross section for the production of two longitudinal W bosons is suppressed by a factor 50 or 100 compared to the full result for $\sqrt{s} = 1\,\text{TeV}$ or $3\,\text{TeV}$, respectively.

The analytical expressions for the $\mathcal{O}(\alpha)$ virtual corrections to WW scattering in the high-energy limit are given in appendix B. The formulas are rather compact and easy to implement. In our default set-up, we have used the version with exact SU(2)-transformed lowest-order matrix elements. This means that we use the complete expression as in (B.21). More precisely, we use (B.27), (B.30), and (B.33). We have verified that the numerical results based on (B.28), (B.31), and (B.34), which are obtained by making use of the high-energy approximation for the SU(2)-transformed Born amplitudes given in appendix D, are in very good agreement. For all results shown in the following, the difference between the two methods is in fact at the per-mille level. This comparison confirms the reliability of the high-energy approximation for the Born matrix elements, under which the correction factor can be factorized and expressed in a very simple form, leading to considerable decrease in CPU time.

In order to estimate the accuracy of the logarithmic high-energy approximation in computing the radiative effects, we have moreover compared our results with the complete $\mathcal{O}(\alpha)$ corrections to the on-shell $W^+_{\lambda_+}W^-_{\lambda_-} \to W^+_{\lambda_5}W^-_{\lambda_6}$ process [38]. For this comparison, we have included the electromagnetic terms given in appendix E, evaluated for a soft-photon cutoff $\Delta E = 0.5\sqrt{\hat{s}}$. In figure 5, we show the difference between the complete $\mathcal{O}(\alpha)$ cross section and the $\mathcal{O}(\alpha)$ result in logarithmic high-energy approximation, normalized to the Born cross section, as a function of the CM energy. The three curves represent the three polarized cross-section differences for $\lambda_+\lambda_-\lambda_5\lambda_6 = \text{TTTT}, \text{LLTT}, \text{TLTL}$, respectively. They all display a plateau at high energy, showing that the difference between approximate and exact result is due to terms that do not grow with energy in that region. This implies that the high-energy behaviour of the radiative effects is well reproduced by the adopted approximation which takes into account only energy-enhanced logarithmic terms.

The terms, omitted in the logarithmic approximation might be, however, not negligible. Figure 5 shows indeed that the agreement between exact and approximate $\mathcal{O}(\alpha)$ cross section is within a few per cent for the first two polarization configurations, while it goes

JHEP03(2007)078

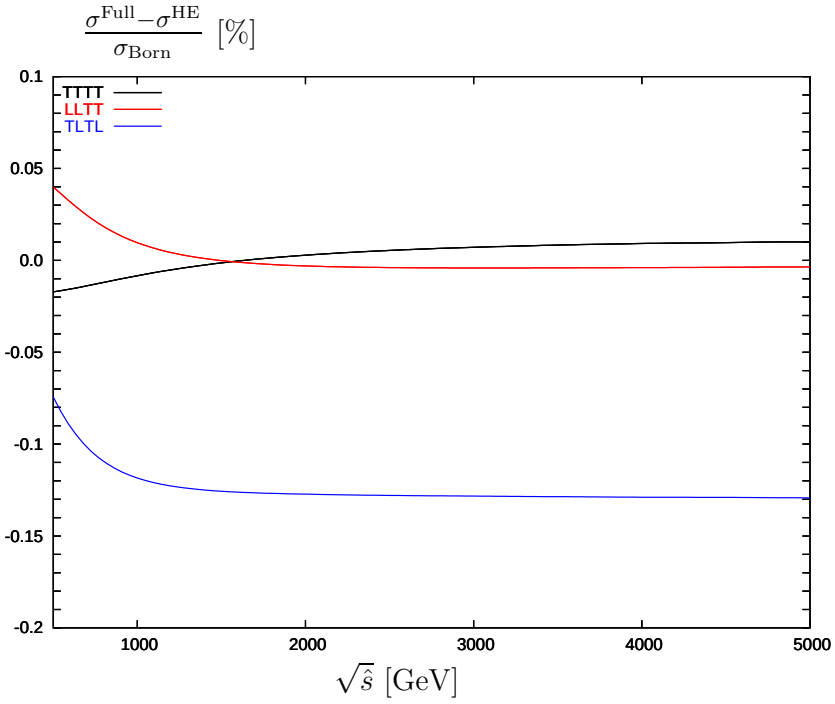

Figure 5: WW-scattering subprocess $W^+_{\lambda_+} W^-_{\lambda_-} \to W^+_{\lambda_5} W^-_{\lambda_6}$. Difference between complete $\mathcal{O}(\alpha)$ cross section (σ^{Full}) and $\mathcal{O}(\alpha)$ cross section in logarithmic high-energy approximation (σ^{HE}), normalized to the lowest-order result. In the legend, T and L refer to the transverse and longitudinal polarizations of the two incoming and two outgoing W bosons from left to right.

up to about 13% for the third one. This discrepancy is unexpectedly large. It could be understood by performing a complete high-energy approximation including non-logarithmic terms. However, for the unpolarized cross section this discrepancy is still tolerable. The lowest-order cross section is in fact dominated by the TTTT configuration, and receives only a 10% contribution from TLTL, as shown in table 2. We can thus safely assume our $\mathcal{O}(\alpha)$ inaccuracy to be of the order of a few per cent.

4. Numerical results

In this section, we illustrate the effect of the logarithmic electroweak corrections on the production of a W^+W^- pair plus missing energy at future e^+e^- colliders. We consider the process (2.1) in the numerical setup given in section 2. We analyse the behaviour of the VBS included in (2.1) over the kinematical region characterized by large diboson invariant masses and large scattering angles of the produced W bosons. This is the domain where possible new-physics effects entering the VBS would be maximally enhanced.

We focus on the SM predictions for a light Higgs boson. As pointed out by Bagger et al. [4], in this case one would observe the production of mostly transversally polarized W bosons in the high WW invariant-mass region. The longitudinal spin configuration is

JHEP03(2007)078

$\sigma(e^+e^- \to \nu_e\bar{\nu}_e W^+W^-)$					
$\sqrt{s}$ [TeV]	σ_{Born} [fb]	σ [fb]	Δ_{EW} [%]	Δ [%]	$1/\sqrt{L\sigma_{\text{Born}}}$ [%]
1	0.595	0.556	−6.7	1.3	4.1
3	3.507	2.897	−17.4	0.2	1.7

Table 3: Total lowest-order cross section (second column) as well as total $\mathcal{O}(\alpha)$ cross section (third column) and electroweak corrections in per cent of the lowest-order result (fourth column), including their uncertainty (fifth column). The last entry shows the statistical error for an integrated luminosity $L = 1\,\text{ab}^{-1}$. Kinematical cuts as in section 2 are applied.

in fact strongly suppressed in the presence of a light Higgs boson. For the specific case at hand, this is shown in table 2 for $M_{\text{H}} = 120\,\text{GeV}$ and two possible setups.

In table 3, we show the impact of the corrections on the total cross section for $e^+e^- \to \nu_e\bar{\nu}_e W^+W^-$ and compare it with the expected statistical error. The second column contains the lowest-order result. The third and fourth entries respectively display the $\mathcal{O}(\alpha)$-corrected cross section and the contribution of the one-loop corrections relative to the Born result, $\Delta_{\text{EW}} = (\sigma - \sigma_{\text{Born}})/\sigma_{\text{Born}}$. The fifth column provides an estimate of the uncertainty of the one-loop contributions due to the EVBA, $\Delta = \Delta_{\text{EW}} \times \Delta_{\text{EVBA}}$, which is obtained combining the one-loop corrections with the uncertainty of the EVBA at Born level. For the considered process, the electroweak radiative effects are negative and of the order of -5% to -20%. This has to be compared with the last column of table 3, where we show an estimate of the statistical error based on an integrated luminosity $L = 1\,\text{ab}^{-1}$. As can be seen, the electroweak corrections are quite important. Already comparable with the statistical uncertainty at the ILC, they further increase at higher energies giving rise to a 10σ effect at CLIC.

The influence of the $\mathcal{O}(\alpha)$ corrections is highly dependent on the cuts imposed and the selected kinematical domain. Also, distributions can be differently affected by the radiative corrections. We illustrate this point for the sample variables defined and analysed in section 3.1. The $\mathcal{O}(\alpha)$ effects on these four observables at $\sqrt{s} = 1\,\text{TeV}$ and $3\,\text{TeV}$ are displayed in figure 6 and figure 7, respectively. The upper curves represent the lowest-order differential cross section, the lower ones the corresponding corrected result.

We first consider the case of $\sqrt{s} = 1\,\text{TeV}$. In the left-upper plot of figure 6, we show the distribution in the diboson invariant mass. This variable, representing the CM energy of the VBS subprocess, gives direct access to the energy scale at which new physics could appear. In absence of a light Higgs boson, the SM VBS amplitudes would violate perturbative unitarity at high CM energies. In order to recover it, new physics should manifest itself at those scales. Hence, at future colliders it will be useful to analyse the diboson production (plus missing energy) at the highest possible $M(\text{WW})$ values. In this region, the $\mathcal{O}(\alpha)$ corrections are enhanced. They can go up to -18%, as shown by the corresponding inset plot. The increase of the radiative effects with $M(\text{WW})$ is a typical effect of large logarithms of Sudakov type. The electroweak corrections should therefore be included to match the experimental accuracy.

JHEP03(2007)078

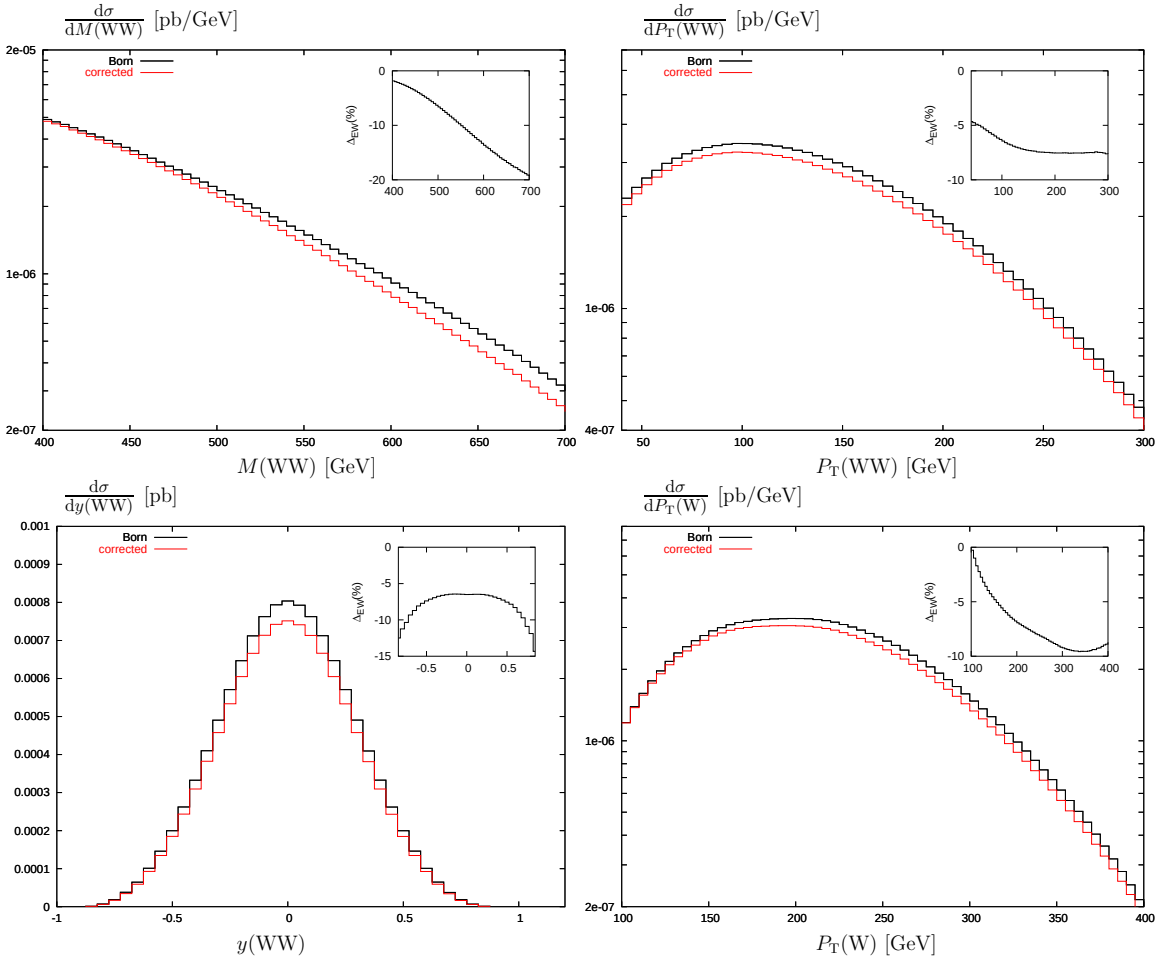

Figure 6: Distributions for $\sqrt{s} = 1\,\text{TeV}$ in lowest order and including logarithmic corrections: invariant mass of the diboson pair (upper left), transverse momentum of the diboson pair (upper right), rapidity of the diboson pair (lower left), transverse momentum of the produced W boson (lower right). The inset plots show the relative $\mathcal{O}(\alpha)$ corrections Δ_{EW} in per cent normalized to the lowest-order results. Standard cuts are applied.

A second variable of interest, $P_{\text{T}}(\text{WW})$, combines energy and angle information. This observable is expected to be sensitive to a strongly interacting VBS signal at low and intermediate values, say for $P_{\text{T}}(\text{WW})$ between 50 and 300 GeV [7]. In this region, the radiative effects are of order -5% to -7%, thus smaller than in the case discussed above. Their size is, however, comparable with the statistical accuracy in the considered range. The same conclusion holds for the pure angular-like variable, $y(\text{WW})$, shown in the left-lower plot, which gets corrections in the range between -7% and -10%. The transverse momentum $P_{\text{T}}(\text{W})$ on the right-lower plot displays instead a behaviour analogous to $M(\text{WW})$. Note that for all considered distributions the corrections reduce the tree-level SM predictions.

In figure 7, we show the same set of distributions as above for $\sqrt{s} = 3\,\text{TeV}$ and the corresponding cuts specified in section 2. As expected the impact of the radiative corrections increases with the collider energy since this allows for higher CM energies, which

JHEP03(2007)078

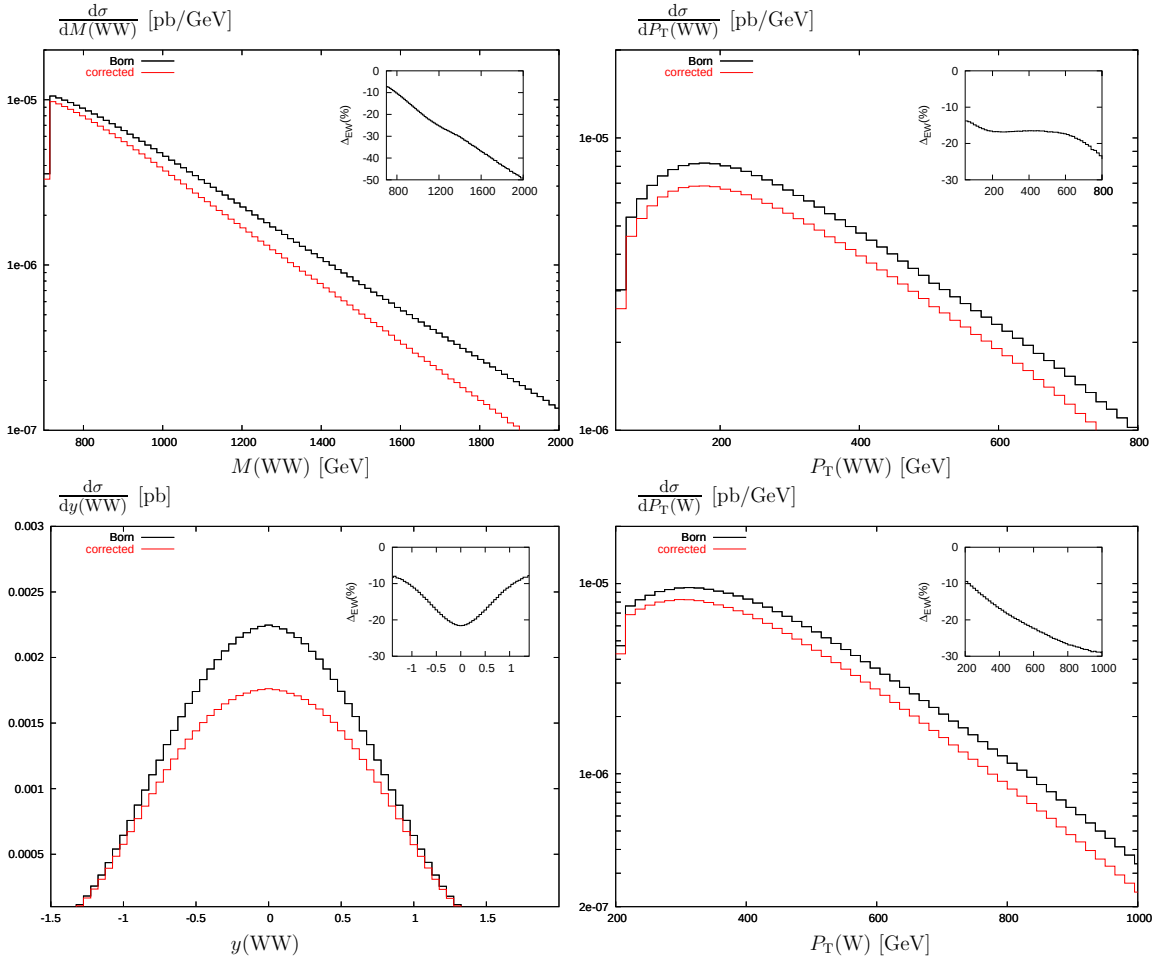

Figure 7: Distributions for 3 TeV in lowest order and including logarithmic corrections. Same conventions as in figure 6.

translate into higher diboson invariant masses and transverse momenta. This behaviour is well depicted in all four plots. For the distributions in $P_{\mathrm{T}}(\mathrm{WW})$ and $y(\mathrm{WW})$ the corrections are in the range between -10% and -20%, apart from the region of very high $P_{\mathrm{T}}(\mathrm{WW})$ where statistics is small. For the $M(\mathrm{WW})$ distribution the electroweak corrections grow from -10% to -50% with increasing invariant mass and for the $P_{\mathrm{T}}(\mathrm{W})$ distribution the effect is similar. For the distribution in $y(\mathrm{WW})$, the corrections are large at the maximum of the distribution at small $y(\mathrm{WW})$. For the other distributions, the cross sections get small where the corrections get large. Still, the $\mathcal{O}(\alpha)$ corrections are statistically relevant. This is illustrated in table 4, where the size of the electroweak corrections Δ_{EW} and the $\mathcal{O}(\alpha)$ uncertainty $\Delta = \Delta_{\mathrm{EW}} \times \Delta_{\mathrm{EVBA}}$, which results from the EVBA, are compared with the statistical accuracy Δ_{stat} based on the projected luminosity $L = 1\,\mathrm{ab}^{-1}$. Dividing the range of energy-like variables in 200 GeV intervals, we find that the influence of the $\mathcal{O}(\alpha)$ corrections is not washed out by the binning. In the more statistically relevant bins, the radiative corrections ranging from -10% to -30% give rise to a 3–6σ effect. In the tails of

JHEP03(2007)078

bin	M(WW)				bin	P_{T}(WW)			
[GeV]	N_{evt}	Δ_{stat}[%]	Δ_{EW}[%]	Δ[%]	[GeV]	N_{evt}	Δ_{stat}[%]	Δ_{EW}[%]	Δ[%]
700–900	1719	2.4	-10.4	0.7	50–250	1467	2.6	-15.9	0.7
900–1100	916	3.3	-18.2	1.2	250–450	1119	3.0	-16.6	2.0
1100–1300	446	4.7	-25.1	1.8	450–650	550	4.3	-17.0	0.5
1300–1500	216	6.8	-30.4	0.7	650–850	249	6.3	-21.4	6.5
1500–1700	106	9.7	-36.8	0.8	850–1050	92	10.4	-32.6	24.9
1700–1900	53	13.7	-43.3	1.5					
1900–2100	26	19.4	-49.5	2.2					
bin	P_{T}(W)				bin	y(WW)			
[GeV]	N_{evt}	Δ_{stat}[%]	Δ_{EW}[%]	Δ[%]		N_{evt}	Δ_{stat}[%]	Δ_{EW}[%]	Δ[%]
200–400	1765	2.4	-13.4	0.9	0–0.25	549	4.3	-21.1	3.2
400–600	1140	3.0	-19.4	1.2	0.25–0.50	486	4.5	-18.9	1.1
600–800	424	4.9	-24.3	3.6	0.50–0.75	374	5.2	-15.6	1.4
800–1000	134	8.6	-27.8	5.5	0.75–1.00	235	6.5	-12.4	3.0
1000–1200	35	16.8	-28.6	8.1	1.00–1.25	101	9.9	-9.9	3.3

Table 4: Impact of electroweak corrections on binned distributions at $\sqrt{s} = 3\,\mathrm{TeV}$. The first and sixth columns show the bin. For each variable, the four entries from left to right give the total number of events for a luminosity $L = 1\,\mathrm{ab}^{-1}$, the corresponding statistical accuracy, the size of the $\mathcal{O}(\alpha)$ electroweak corrections relative to the Born result, and the estimated one-loop uncertainty due to the EVBA.

bin	M(WW)				bin	P_{T}(WW)			
[GeV]	N_{evt}	Δ_{stat}[%]	Δ_{EW}[%]	Δ[%]	[GeV]	N_{evt}	Δ_{stat}[%]	Δ_{EW}[%]	Δ[%]
400–500	363	5.2	-3.5	1.0	40–140	316	5.6	-6.1	1.3
500–600	157	8.0	-9.4	1.1	140–240	215	6.8	-7.4	1.6
600–700	57	13.2	-16.0	0.5	240–340	59	13.0	-7.6	0.5
700–800	16	24.8	-19.9	2.0					
bin	P_{T}(W)				bin	y(WW)			
[GeV]	N_{evt}	Δ_{stat}[%]	Δ_{EW}[%]	Δ[%]		N_{evt}	Δ_{stat}[%]	Δ_{EW}[%]	Δ[%]
100–200	259	6.2	-4.8	0.7	0–0.25	180	7.4	-6.5	0.7
200–300	259	6.2	-7.9	1.6	0.25–0.50	94	10.3	-6.9	2.1
300–400	72	11.8	-9.4	3.1	0.50–0.75	23	20.8	-8.3	3.8

Table 5: Impact of electroweak corrections on binned distributions at $\sqrt{s} = 1\,\mathrm{TeV}$. Same conventions as in table 4.

the distributions, the $\mathcal{O}(\alpha)$ contributions can increase up to -50%, still being bigger than the estimated experimental accuracy. We also observe that, apart from the region of very high P_{T}(WW), the uncertainty associated with the EVBA never exceeds the statistical error.

JHEP03(2007)078

In table 5 we give analogous results for $\sqrt{s} = 1\,\text{TeV}$. In this case, the radiative effects are comparable with the statistical accuracy. Their significance is strictly dependent on the binning.

In our analysis, we have not included any option on the polarization of the initial beams. In the process $e^+e^- \to \nu_e\bar{\nu}_e W^+W^-$, the VBS signal is purely given by the W-boson scattering, as illustrated in the first Feynman diagram of figure 1. Only the right-left combination $e^+_R e^-_L$ thus contributes to the signal. The irreducible background (see for instance the last diagram in figure 1) can receive instead contributions also from other helicity configurations. The possibility of selecting a given initial polarization has thus two advantages. In first place, it helps in suppressing the background. As a second benefit, it increases the statistics. Assuming a polarization efficiency of 80% and 60% for electron and positron, respectively, we would have in fact an increase of about a factor two in the number of events at fixed luminosity. In this set-up, the relevance of the radiative effects would be further enhanced.

5. Conclusions

If the Higgs boson should be heavy or absent, the scattering of longitudinal electroweak gauge bosons can provide information on the mechanism of electroweak symmetry breaking. An irreducible background to signals of new physics in vector-boson scattering is provided by the Standard Model contribution for a light Higgs boson. In order to be able to disentangle possible small new-physics effects a precise knowledge of the latter is required.

We have studied electroweak radiative corrections to W^+W^- scattering at high-energy e^+e^- colliders. We have used the equivalent vector-boson approximation and calculated the factorizable one-loop corrections in the high-energy logarithmic approximation. Corrections to the splitting of the W bosons from the incoming particles as well as non-factorizable corrections have not been taken into account. We have presented explicit analytical results for the logarithmic corrections to $W^+W^- \to W^+W^-$. These have been implemented into a Monte Carlo program for the process $e^+e^- \to \nu_e\bar{\nu}_e W^+W^-$ together with the complete lowest-order matrix elements.

We have defined a set of cuts suitable for the analysis of the scattering of strongly interacting W bosons and investigated our approximations within this setup. In kinematical regions that are statistically relevant and receive non-negligible corrections, we find that the effective vector-boson approximation agrees with the complete lowest-order prediction within about 20% to 25%. The logarithmic approximation reproduces the complete one-loop corrections for the unpolarized cross section of $W^+W^- \to W^+W^-$ at the level of a few per cent. These approximations cause an uncertainty of our predictions at the level of a few per cent. This uncertainty is always comparable to the statistical error. In principle it can be further reduced by introducing appropriate cuts that improve the accuracy of the EVBA. But, in general, for a given set of cuts, a better precision can be achieved only by means of an exact calculation.

JHEP03(2007)078

The size of the electroweak corrections depends strongly on the cuts and the considered observable. We have studied their effect on the total cross section and four physically interesting distributions. Within our set-up, the corrections to the total cross section amount to -7% and -17% for $\sqrt{s} = 1\,\text{TeV}$ and $\sqrt{s} = 3\,\text{TeV}$, respectively. For the distributions in the transverse momentum and the rapidity of the W-boson pair they are of similar size. In the distributions in the invariant mass of the W-boson pair and the transverse momentum of a W boson, the corrections are negative, of the order of 10% and increase in magnitude with increasing energy. They can reach up to -20% and -50% for $\sqrt{s} = 1\,\text{TeV}$ and $\sqrt{s} = 3\,\text{TeV}$, respectively. In summary, the electroweak corrections reduce the Standard Model predictions by a sizeable amount that is comparable or larger than the expected statistical error. Therefore, they should be taken into account when searching for effects of a strongly interacting scalar sector. In fact, being negative, the corrections increase the sensitivity to this kind of effects, which typically appear as an enhancement of the WW-scattering cross section.

Acknowledgments

This work was supported by the Italian Ministero dell'Istruzione, dell'Università e della Ricerca (MIUR) under contract Decreto MIUR 26-01-2001 N.13 "Incentivazione alla mobilità di studiosi stranieri ed italiani residenti all'estero".

A. On-shell projection

In this section we give the explicit form of the on-shell projection of the two incoming W bosons which induce the VBS. When performing the projection, care should be taken that the on-shell projected W-boson momenta lie in the physical phase-space region. This can be ensured by fixing the angles of the two incoming bosons while performing their on-shell limit. We thus fix the direction of the incoming W^+ in the CM frame of the W-boson pair. In this way, the on-shell projected momenta can be written as

$$\hat{q}_{\pm}^{\text{on}} = \frac{\sqrt{\hat{s}}}{2}\left(1, \pm\beta\frac{\hat{\mathbf{q}}_+}{|\hat{\mathbf{q}}_+|}\right), \tag{A.1}$$

where $\sqrt{\hat{s}}$ is the VBS CM energy, $\beta = \sqrt{1 - 4M_{\mathrm{W}}^2/\hat{s}}$, and $\hat{\mathbf{q}}_+$ is the three-momentum of the incoming (off-shell) W^+ boson in the CM frame of the W-boson pair. The on-shell momenta are then boosted to the laboratory frame.

B. Logarithmic electroweak corrections

In this appendix, using the general results of refs. [12, 14], we derive analytical formulas for the logarithmic electroweak corrections to the subprocess

$$\mathrm{W}^-_{\lambda_1}(k_1)\mathrm{W}^+_{\lambda_2}(k_2) \to \mathrm{W}^-_{-\lambda_3}(-k_3)\mathrm{W}^+_{-\lambda_4}(-k_4). \tag{B.1}$$

JHEP03(2007)078

The momenta k_3, k_4 and the helicities λ_3, λ_4 of the final states are defined as incoming. The $2 \to 2$ process (B.1) is thus equivalent to the $4 \to 0$ process

$$\mathrm{W}^-_{\lambda_1}(k_1)\mathrm{W}^+_{\lambda_2}(k_2)\mathrm{W}^+_{\lambda_3}(k_3)\mathrm{W}^-_{\lambda_4}(k_4) \to 0. \tag{B.2}$$

This convention facilitates the application of the formalism of refs. [12, 14], which is based on $n \to 0$ reactions. We consider the limit of high energies and large scattering angles, where all invariants are much larger than the electroweak scale,

$$|r_{ij}| = |(k_i + k_j)^2| \simeq |2k_i k_j| \gg M_{\mathrm{W}}^2 \qquad \text{for} \quad i \neq j. \tag{B.3}$$

In order to specify our conventions for the gauge-boson helicities, which we denote by $\lambda_i = 0, \pm 1$, we choose the CM frame. There, the gauge-boson momenta can be parametrized as

$$\begin{aligned} k_1^\mu &= E(1,0,0,1), & -k_3^\mu &= E(1,\sin\vartheta,0,\cos\vartheta), \\ k_2^\mu &= E(1,0,0,-1), & -k_4^\mu &= E(1,-\sin\vartheta,0,-\cos\vartheta), \end{aligned} \tag{B.4}$$

and for the Mandelstam variables we have $r_{12} = r_{34} = 4E^2$, $r_{13} = r_{24} = -r_{12}(1-\cos\vartheta)/2$, $r_{23} = r_{14} = -r_{12}(1+\cos\vartheta)/2$. Note that mass terms are systematically neglected in the high-energy limit. The polarization vectors for transverse gauge bosons ($\lambda_i = \tau_i = \pm 1$) read

$$\begin{aligned} \varepsilon^\mu(k_1,\tau_1) &= \frac{1}{\sqrt{2}}(0,1,\tau_1\mathrm{i},0), & \varepsilon^{\mu*}(-k_3,-\tau_3) &= \frac{1}{\sqrt{2}}(0,\cos\vartheta,\tau_3\mathrm{i},-\sin\vartheta), \\ \varepsilon^\mu(k_2,\tau_2) &= \frac{1}{\sqrt{2}}(0,-1,\tau_2\mathrm{i},0), & \varepsilon^{\mu*}(-k_4,-\tau_4) &= \frac{1}{\sqrt{2}}(0,-\cos\vartheta,\tau_4\mathrm{i},\sin\vartheta). \end{aligned} \tag{B.5}$$

Here and in the following, the symbol $\tau_i = \pm 1$ is used to denote the helicity of transversely polarized gauge bosons. Longitudinal gauge bosons ($\lambda_i = 0$) have to be related to corresponding would-be Goldstone bosons using the Goldstone Boson Equivalence Theorem (GBET) as discussed in appendix C. There, we also introduce effective couplings for longitudinal gauge bosons, which permit to apply the general results of ref. [12] directly to physical matrix elements.

The matrix element for the process (B.1) or, equivalently, (B.2) is denoted as

$$\mathcal{M}^{W^-_{\lambda_1}W^+_{\lambda_2}W^+_{\lambda_3}W^-_{\lambda_4}} \equiv \mathcal{M}^{W^-_{\lambda_1}W^+_{\lambda_2}W^+_{\lambda_3}W^-_{\lambda_4}}(r_{12}, r_{13}, r_{23}). \tag{B.6}$$

In the high-energy limit, we restrict ourselves to the matrix elements that are not mass-suppressed by factors of order $M_{\mathrm{W}}/\sqrt{r_{12}}$. By means of the GBET, it can easily be seen that only the matrix elements involving helicity combinations with an even number of longitudinally (L) and transversely (T) polarized gauge bosons are not suppressed. The reason is that all vertices involving an odd number of Goldstone bosons are suppressed by coupling factors proportional to masses. In addition, the matrix elements with helicities TL $\to$ LT and LT $\to$ TL are suppressed, i.e.

$$\mathcal{M}^{W^-_{\tau_1}W^+_0W^+_0W^-_{\tau_4}} = \mathcal{M}^{W^-_0W^+_{\tau_2}W^+_{\tau_3}W^-_0} = 0, \tag{B.7}$$

JHEP03(2007)078

up to terms of order M_{W}^2/r_{12}. Therefore, in the following we restrict ourselves to the non-suppressed combinations

$$\begin{aligned}
\mathrm{LL}\to\mathrm{LL}:&\ \mathrm{W}_0^-\mathrm{W}_0^+\to\mathrm{W}_0^-\mathrm{W}_0^+,\\
\mathrm{TT}\to\mathrm{LL}:&\ \mathrm{W}_{\tau_1}^-\mathrm{W}_{\tau_2}^+\to\mathrm{W}_0^-\mathrm{W}_0^+,\\
\mathrm{LL}\to\mathrm{TT}:&\ \mathrm{W}_0^-\mathrm{W}_0^+\to\mathrm{W}_{-\tau_3}^-\mathrm{W}_{-\tau_4}^+,\\
\mathrm{TL}\to\mathrm{TL}:&\ \mathrm{W}_{\tau_1}^-\mathrm{W}_0^+\to\mathrm{W}_{-\tau_3}^-\mathrm{W}_0^+,\\
\mathrm{LT}\to\mathrm{LT}:&\ \mathrm{W}_0^-\mathrm{W}_{\tau_2}^+\to\mathrm{W}_0^-\mathrm{W}_{-\tau_4}^+,\\
\mathrm{TT}\to\mathrm{TT}:&\ \mathrm{W}_{\tau_1}^-\mathrm{W}_{\tau_2}^+\to\mathrm{W}_{-\tau_3}^-\mathrm{W}_{-\tau_4}^+.
\end{aligned}\tag{B.8}$$

The amplitudes for LL $\to$ TT, TL $\to$ TL, and LT $\to$ LT can be obtained from the amplitude TT $\to$ LL using the relations

$$\begin{aligned}
\mathcal{M}^{W_0^-W_0^+W_{\tau_3}^+W_{\tau_4}^-} &= \mathcal{M}^{W_{\tau_4}^-W_{\tau_3}^+W_0^+W_0^-},\\
\mathcal{M}^{W_{\tau_1}^-W_0^+W_{\tau_3}^+W_0^-} &= \mathcal{M}^{W_{\tau_1}^-W_{\tau_3}^+W_0^+W_0^-}\Big|_{r_{12}\leftrightarrow r_{13}},\\
\mathcal{M}^{W_0^-W_{\tau_2}^+W_0^+W_{\tau_4}^-} &= \mathcal{M}^{W_{\tau_4}^-W_{\tau_2}^+W_0^+W_0^-}\Big|_{r_{12}\leftrightarrow r_{13}},
\end{aligned}\tag{B.9}$$

which follow from crossing symmetry.

B.1 Structure of the one-loop logarithmic corrections

In the following sections, our results for the one-loop logarithmic corrections are given either in explicit form, or as correction factors

$$\delta_{\mathrm{W}_{\lambda_1}^-\mathrm{W}_{\lambda_2}^+\to\mathrm{W}_{-\lambda_3}^-\mathrm{W}_{-\lambda_4}^+}=\frac{\delta\mathcal{M}_1^{W_{\lambda_1}^-W_{\lambda_2}^+W_{\lambda_3}^+W_{\lambda_4}^-}}{\mathcal{M}_0^{W_{\lambda_1}^-W_{\lambda_2}^+W_{\lambda_3}^+W_{\lambda_4}^-}},\tag{B.10}$$

relative to the Born matrix elements. Following ref. [12], we split the logarithmic corrections (B.10) according to their origin as

$$\delta=\delta^{\mathrm{LSC}}+\delta^{\mathrm{SSC}}+\delta^{\mathrm{C}}+\delta^{\mathrm{PR}}.\tag{B.11}$$

The double logarithms originating from soft-collinear gauge bosons are split into leading contributions δ^{LSC} of the type $\alpha\log^2(|r_{12}|/M^2)$ and subleading contributions δ^{SSC} of the type $\alpha\log(|r_{12}|/M^2)\log(|r_{ij}/r_{12}|)$, with $r_{ij}=r_{13},r_{23}$. These latter depend on ratios of Mandelstam variables, $|r_{13}/r_{12}|=(1-\cos\vartheta)/2$, $|r_{23}/r_{12}|=(1+\cos\vartheta)/2$, and thus on the scattering angle ϑ between initial and final states. Purely angular-dependent logarithms of the type $\alpha\log^2(|r_{ij}/r_{12}|)$ and $\alpha\log(|r_{ij}/r_{12}|)$ are neglected in our approximation. The part δ^{C} contains the single-logarithmic contributions from collinear (or soft) particles to loop diagrams and wave-function renormalization constants. Finally, δ^{PR} consists of the single logarithms that originate from parameter renormalization.

All these logarithmic contributions depend on various mass scales M=M_{W}, M_{Z}, M_γ, M_{H}, m_{t}. This mass dependence is separated from the energy dependence by writing

$$\log\left(\frac{|r_{ij}|}{M^2}\right)=\log\left(\frac{|r_{ij}|}{M_{\mathrm{W}}^2}\right)-\log\left(\frac{M^2}{M_{\mathrm{W}}^2}\right),\tag{B.12}$$

JHEP03(2007)078

i.e. we split all logarithms into a contribution with scale $M_{\rm W}$ and a remaining part that depends on the ratio $M^2/M_{\rm W}^2$. The logarithms of $m_{\rm t}/M_{\rm W}$ and $M_{\rm H}/M_{\rm W}$ can be found in ref. [14]. Here we give all logarithms of $m_{\rm t}/M_{\rm W}$ as well as the universal logarithms of $M_{\rm H}/M_{\rm W}$, i.e. those that originate from parameter renormalization and collinear singularities. Also the subleading logarithms of the type $\alpha \log(|r_{12}|/M_{\rm W}^2) \log(M_{\rm Z}^2/M_{\rm W}^2)$ are included.

In ref. [12], the virtual electromagnetic corrections have been regularized by an infinitesimal photon mass $M_\gamma = \lambda$ and split as in (B.12) into a contribution corresponding to a heavy photon ($\lambda = M_{\rm W}$) and a remaining part which originates from the mass gap $\lambda \ll M_{\rm W}$ in the gauge sector. The heavy-photon contribution has been combined with the weak corrections resulting into the so-called symmetric-electroweak part of the corrections. The remaining mass-gap contribution has been isolated into the infrared-divergent logarithms $L^{\rm em}(s, \lambda^2, m_k^2)$, $l(M_{\rm W}^2, \lambda^2)$, $l^{\rm em}(m_k^2)$ which appear in eqs. (3.7), (3.8), (3.10), (3.12), (4.6), (4.7), (4.10) and (4.33) of ref. [12]. These logarithms contain only contributions from virtual photons.

In appendix E we provide simple substitutions that permit to generalize the results of ref. [12] to semi-inclusive $2 \to 2$ processes, by including the soft-photon bremsstrahlung corrections. The resulting logarithms, defined in (E.1), (E.2), and (E.3), are infrared finite and depend on the soft-photon cutoff ΔE.

Notation. The coefficients of the various logarithms are expressed in terms of the eigenvalues $I_\varphi^{V^a}$, or of the matrix components $I_{\varphi\varphi'}^{V^a}$, of the generators[2]

$$I^A = -Q = -\frac{Y}{2} - T^3, \qquad I^Z = -\frac{s_{\rm W}}{c_{\rm W}}\frac{Y}{2} + \frac{c_{\rm W}}{s_{\rm W}} T^3, \qquad I^{W^\pm} = \frac{T^1 \pm {\rm i} T^2}{\sqrt{2} s_{\rm W}}, \tag{B.13}$$

where $c_{\rm W}^2 = 1 - s_{\rm W}^2 = M_{\rm W}^2/M_{\rm Z}^2$. Another group-theoretical object that often appears in our results is the electroweak Casimir operator

$$C^{\rm ew} = \sum_{V^a = A, Z, W^\pm} I^{V^a} I^{\bar{V}^a} = \frac{1}{c_{\rm W}^2} \left(\frac{Y}{2}\right)^2 + \frac{1}{s_{\rm W}^2} T(T+1), \tag{B.14}$$

where T represents the total isospin.

B.2 Leading soft-collinear corrections

Below we list the angular-independent leading soft-collinear (LSC) corrections for various polarizations of the gauge bosons. These results are obtained from eqs. (3.6) and (3.7) of ref. [12] and depend on the eigenvalues of the electroweak Casimir operator

$$C_\Phi^{\rm ew} = \frac{1 + 2c_{\rm W}^2}{4 s_{\rm W}^2 c_{\rm W}^2}, \qquad C_W^{\rm ew} = \frac{2}{s_{\rm W}^2}, \tag{B.15}$$

[2] A detailed list of the gauge-group generators and of related quantities that are used in the following can be found in appendix B of ref. [12] and appendix B of ref. [14].

JHEP03(2007)078

as well as on the squared Z-boson couplings

$$(I^Z_{W^\pm})^2 = \frac{c_{\rm W}^2}{s_{\rm W}^2}, \qquad (I^Z_{\phi^\pm})^2 = \frac{(c_{\rm W}^2 - s_{\rm W}^2)^2}{4 s_{\rm W}^2 c_{\rm W}^2}. \tag{B.16}$$

The explicit expressions for the electromagnetic logarithms $L^{\rm EM}(M_{\rm W}^2)$, which contain contributions from both virtual and real soft photons, are given in (E.1).

Purely longitudinal polarizations.

$$\begin{aligned}\delta^{\rm LSC}_{{\rm W}^-_0{\rm W}^+_0\to{\rm W}^-_0{\rm W}^+_0} = &-\frac{\alpha}{2\pi}\left[C^{\rm ew}_\Phi \log^2\left(\frac{|r_{12}|}{M_{\rm W}^2}\right) - 2\left(I^Z_{\phi^\pm}\right)^2 \log\left(\frac{M_{\rm Z}^2}{M_{\rm W}^2}\right)\log\left(\frac{|r_{12}|}{M_{\rm W}^2}\right)\right] \\ &- 2L^{\rm EM}(M_{\rm W}^2).\end{aligned} \tag{B.17}$$

Mixed polarizations.

$$\begin{aligned}\delta^{\rm LSC}_{{\rm W}^-_{\tau_1}{\rm W}^+_{\tau_2}\to{\rm W}^-_0{\rm W}^+_0} &= \delta^{\rm LSC}_{{\rm W}^-_0{\rm W}^+_0\to{\rm W}^-_{-\tau_3}{\rm W}^+_{-\tau_4}} = \delta^{\rm LSC}_{{\rm W}^-_{\tau_1}{\rm W}^+_0\to{\rm W}^-_{-\tau_3}{\rm W}^+_0} = \delta^{\rm LSC}_{{\rm W}^-_0{\rm W}^+_{\tau_2}\to{\rm W}^-_0{\rm W}^+_{-\tau_4}} = \\ &= -\frac{\alpha}{4\pi}\left[(C^{\rm ew}_W + C^{\rm ew}_\Phi)\log^2\left(\frac{|r_{12}|}{M_{\rm W}^2}\right)\right. \\ &\quad \left. - 2\left[\left(I^Z_{W^\pm}\right)^2 + \left(I^Z_{\phi^\pm}\right)^2\right]\log\left(\frac{M_{\rm Z}^2}{M_{\rm W}^2}\right)\log\left(\frac{|r_{12}|}{M_{\rm W}^2}\right)\right] - 2L^{\rm EM}(M_{\rm W}^2).\end{aligned} \tag{B.18}$$

Purely transverse polarizations.

$$\begin{aligned}\delta^{\rm LSC}_{{\rm W}^-_{\tau_1}{\rm W}^+_{\tau_2}\to{\rm W}^-_{-\tau_3}{\rm W}^+_{-\tau_4}} = &-\frac{\alpha}{2\pi}\left[C^{\rm ew}_W \log^2\left(\frac{|r_{12}|}{M_{\rm W}^2}\right) - 2\left(I^Z_{W^\pm}\right)^2 \log\left(\frac{M_{\rm Z}^2}{M_{\rm W}^2}\right)\log\left(\frac{|r_{12}|}{M_{\rm W}^2}\right)\right] \\ &- 2L^{\rm EM}(M_{\rm W}^2).\end{aligned} \tag{B.19}$$

B.3 Subleading soft-collinear corrections

The angular-dependent subleading soft-collinear (SSC) corrections to the $2 \to 2$ processes (B.8) are obtained by applying the formula (3.12) of ref. [12] [see also (C.2)] to the corresponding $4 \to 0$ processes which result from reversing the outgoing particles by a crossing transformation, i.e. the charges of the outgoing states have to be reversed as in (B.6). The corrections to matrix elements involving longitudinal gauge bosons are obtained via the GBET applying eq. (3.12) of ref. [12] to corresponding matrix elements that involve would-be Goldstone bosons. Alternatively, as discussed in appendix C, one can directly apply eq. (3.12) of ref. [12] to matrix elements for longitudinal gauge bosons using the effective couplings (C.3).

The SSC corrections originating from soft neutral gauge bosons $N = A, Z$ result in

$$\begin{aligned}\sum_{N=A,Z}\delta^{N,\rm SSC}_{{\rm W}^-_{\lambda_1}{\rm W}^+_{\lambda_2}\to{\rm W}^-_{-\lambda_3}{\rm W}^+_{-\lambda_4}} = &\frac{\alpha}{2\pi}\log\left(\frac{|r_{12}|}{M_{\rm W}^2}\right)\sum_{N=A,Z}\left[\left(I^N_{W^-_{\lambda_1}}I^N_{W^+_{\lambda_3}} + I^N_{W^+_{\lambda_2}}I^N_{W^-_{\lambda_4}}\right)\log\left(\frac{|r_{13}|}{|r_{12}|}\right)\right. \\ &\left. + \left(I^N_{W^-_{\lambda_1}}I^N_{W^-_{\lambda_4}} + I^N_{W^+_{\lambda_2}}I^N_{W^+_{\lambda_3}}\right)\log\left(\frac{|r_{23}|}{|r_{12}|}\right)\right] - 4\log\left(\frac{|r_{13}|}{|r_{23}|}\right) l^{\rm EM}_{\rm SSC},\end{aligned} \tag{B.20}$$

JHEP03(2007)078

where the couplings $I^N_{W_0^\pm}$ for longitudinal gauge bosons are given in (C.13), whereas for transverse gauge bosons $I^A_{W_\tau^\pm} = \mp 1$ and $I^Z_{W_\tau^\pm} = \pm c_\mathrm{W}/s_\mathrm{W}$. The electromagnetic logarithms $l^\mathrm{EM}_\mathrm{SSC}$ are defined in (E.2).

Soft virtual W bosons can be exchanged only in the r_{13} channel, and yield

$$\sum_{V=W^\pm} \delta^{V,\mathrm{SSC}} \mathcal{M}^{W^-_{\lambda_1} W^+_{\lambda_2} W^+_{\lambda_3} W^-_{\lambda_4}} = \frac{\alpha}{2\pi} \log\left(\frac{|r_{12}|}{M^2_\mathrm{W}}\right) \log\left(\frac{|r_{13}|}{|r_{12}|}\right) \times \left[\sum_{N_{\lambda_1}} \sum_{N'_{\lambda_3}} J^-_{N_{\lambda_1}} J^+_{N'_{\lambda_3}} \mathcal{M}_0^{N_{\lambda_1} W^+_{\lambda_2} N'_{\lambda_3} W^-_{\lambda_4}} + \sum_{N_{\lambda_2}} \sum_{N'_{\lambda_4}} J^+_{N_{\lambda_2}} J^-_{N'_{\lambda_4}} \mathcal{M}_0^{W^-_{\lambda_1} N_{\lambda_2} W^+_{\lambda_3} N'_{\lambda_4}}\right], \quad \text{(B.21)}$$

where the sums over N_λ and N'_λ depend on the polarization λ. In the case $\lambda = 0$, they run over $N_0 = H, Z_0$, whereas for $\lambda = \tau = \pm 1$ they run over $N_\tau = A_\tau, Z_\tau$. The corresponding couplings $J^\pm_H, J^\pm_{Z_0}$ and $J^\pm_{A_\tau}, J^\pm_{Z_\tau}$ are given in (C.15) and (C.16), respectively. The SU(2)-transformed Born matrix elements that appear on the right-hand side of (B.21) are evaluated in the high-energy limit in appendix D.

In the following we list the explicit results corresponding to all helicity combinations (B.8). Note that, owing to crossing symmetry, both contributions (B.20) and (B.21) are invariant with respect to simultaneous exchange of the polarizations $\lambda_1 \leftrightarrow \lambda_4, \lambda_2 \leftrightarrow \lambda_3$, i.e.

$$\begin{aligned} \sum_{N=A,Z} \delta^{N,\mathrm{SSC}}_{\mathrm{W}^-_{\lambda_4}\mathrm{W}^+_{\lambda_3}\to\mathrm{W}^-_{-\lambda_2}\mathrm{W}^+_{-\lambda_1}} &= \sum_{N=A,Z} \delta^{N,\mathrm{SSC}}_{\mathrm{W}^-_{\lambda_1}\mathrm{W}^+_{\lambda_2}\to\mathrm{W}^-_{-\lambda_3}\mathrm{W}^+_{-\lambda_4}}, \\ \sum_{V=W^\pm} \delta^{V,\mathrm{SSC}} \mathcal{M}^{W^-_{\lambda_4} W^+_{\lambda_3} W^+_{\lambda_2} W^-_{\lambda_1}} &= \sum_{V=W^\pm} \delta^{V,\mathrm{SSC}} \mathcal{M}^{W^-_{\lambda_1} W^+_{\lambda_2} W^+_{\lambda_3} W^-_{\lambda_4}}. \end{aligned} \quad \text{(B.22)}$$

Therefore, the corrections for LL → TT and LT → LT can easily be obtained from those for TT → LL and TL → TL, respectively.

Purely longitudinal polarizations. The contribution (B.20) of soft neutral gauge bosons gives

$$\sum_{N=A,Z} \delta^{N,\mathrm{SSC}}_{\mathrm{W}^-_0\mathrm{W}^+_0\to\mathrm{W}^-_0\mathrm{W}^+_0} = -\frac{\alpha}{4\pi s^2_\mathrm{W} c^2_\mathrm{W}} \log\left(\frac{|r_{12}|}{M^2_\mathrm{W}}\right) \log\left(\frac{|r_{13}|}{|r_{23}|}\right) - 4 \log\left(\frac{|r_{13}|}{|r_{23}|}\right) l^\mathrm{EM}_\mathrm{SSC}. \quad \text{(B.23)}$$

The contribution (B.21) of soft W bosons yields

$$\begin{aligned} &\sum_{V=W^\pm} \delta^{V,\mathrm{SSC}} \mathcal{M}^{W^-_0 W^+_0 W^+_0 W^-_0} = \\ &= \frac{\alpha}{2\pi} \log\left(\frac{|r_{12}|}{M^2_\mathrm{W}}\right) \log\left(\frac{|r_{13}|}{|r_{12}|}\right) \sum_{S,S'=H,Z_0} J^-_S J^+_{S'} \left[\mathcal{M}_0^{S W^+_0 S' W^-_0} + \mathcal{M}_0^{W^-_0 S' W^+_0 S}\right] \\ &= \frac{\alpha}{8\pi s^2_\mathrm{W}} \log\left(\frac{|r_{12}|}{M^2_\mathrm{W}}\right) \log\left(\frac{|r_{13}|}{|r_{12}|}\right) \left\{\left[\left(\mathcal{M}_0^{H W^+_0 H W^-_0} + \mathcal{M}_0^{W^-_0 H W^+_0 H}\right) - (H \to Z_0)\right]\right. \\ &\quad \left. - \left[\left(\mathcal{M}_0^{H W^+_0 Z_0 W^-_0} + \mathcal{M}_0^{W^-_0 Z_0 W^+_0 H}\right) - (H \leftrightarrow Z_0)\right]\right\}. \end{aligned} \quad \text{(B.24)}$$

JHEP03(2007)078

Using our expressions (D.7), (D.8) for the SU(2)-transformed Born matrix elements in the high-energy limit, and dividing by the Born matrix element (D.6) we obtain

$$\sum_{V=W^\pm} \delta^{V,\mathrm{SSC}}_{\mathrm{W}_0^-\mathrm{W}_0^+\to\mathrm{W}_0^-\mathrm{W}_0^+} = -\frac{\alpha}{2\pi s_\mathrm{W}^2}\log\left(\frac{|r_{12}|}{M_\mathrm{W}^2}\right)\log\left(\frac{|r_{13}|}{|r_{12}|}\right)\left[\frac{\lambda_\mathrm{H}}{2}+\frac{e^2}{2s_\mathrm{W}^2}\frac{r_{13}-r_{23}}{r_{12}}\right. \\ \left.+e^2\frac{s_\mathrm{W}^2-c_\mathrm{W}^2}{4s_\mathrm{W}^2c_\mathrm{W}^2}\frac{r_{12}-r_{23}}{r_{13}}\right]\left[\lambda_\mathrm{H}+\frac{e^2}{4s_\mathrm{W}^2c_\mathrm{W}^2}\left(\frac{r_{13}-r_{23}}{r_{12}}+\frac{r_{12}-r_{23}}{r_{13}}\right)\right]^{-1}, \tag{B.25}$$

where λ_H is the scalar self coupling defined in (D.5).

Mixed polarizations: TT → LL and LL → TT. For the TT → LL configuration, the contribution (B.20) of soft neutral gauge bosons gives

$$\sum_{N=A,Z} \delta^{N,\mathrm{SSC}}_{\mathrm{W}_{\tau_1}^-\mathrm{W}_{\tau_2}^+\to\mathrm{W}_0^-\mathrm{W}_0^+} = -\frac{\alpha}{2\pi s_\mathrm{W}^2}\log\left(\frac{|r_{12}|}{M_\mathrm{W}^2}\right)\log\left(\frac{|r_{13}|}{|r_{23}|}\right)-4\log\left(\frac{|r_{13}|}{|r_{23}|}\right)l^{\mathrm{EM}}_{\mathrm{SSC}}. \tag{B.26}$$

Soft virtual W bosons (B.21) yield

$$\sum_{V=W^\pm}\delta^{V,\mathrm{SSC}}\mathcal{M}^{W_{\tau_1}^-W_{\tau_2}^+W_0^+W_0^-} = \\ = \frac{\alpha}{2\pi}\log\left(\frac{|r_{12}|}{M_\mathrm{W}^2}\right)\log\left(\frac{|r_{13}|}{|r_{12}|}\right)\sum_{N=A,Z}\sum_{S=H,Z_0}\left[J_N^-J_S^+\mathcal{M}_0^{N_{\tau_1}W_{\tau_2}^+SW_0^-}+J_N^+J_S^-\mathcal{M}_0^{W_{\tau_1}^-N_{\tau_2}W_0^+S}\right] \\ = \frac{\alpha}{4\pi s_\mathrm{W}}\log\left(\frac{|r_{12}|}{M_\mathrm{W}^2}\right)\log\left(\frac{|r_{13}|}{|r_{12}|}\right)\left\{\left[-\mathcal{M}_0^{A_{\tau_1}W_{\tau_2}^+HW_0^-}+\mathcal{M}_0^{W_{\tau_1}^-A_{\tau_2}W_0^+H}\right.\right. \\ \left.\left.+\mathcal{M}_0^{A_{\tau_1}W_{\tau_2}^+Z_0W_0^-}+\mathcal{M}_0^{W_{\tau_1}^-A_{\tau_2}W_0^+Z_0}\right]-\frac{c_\mathrm{W}}{s_\mathrm{W}}\left[A\to Z\right]\right\}. \tag{B.27}$$

Using the Born amplitudes (D.11), (D.12) in the high-energy limit we obtain the relative correction

$$\sum_{V=W^\pm}\delta^{V,\mathrm{SSC}}_{\mathrm{W}_{\tau_1}^-\mathrm{W}_{\tau_2}^+\to\mathrm{W}_0^-\mathrm{W}_0^+} = \frac{\alpha}{2\pi s_\mathrm{W}^2}\left(\frac{r_{13}}{r_{23}}-1\right)\log\left(\frac{|r_{12}|}{M_\mathrm{W}^2}\right)\log\left(\frac{|r_{13}|}{|r_{12}|}\right). \tag{B.28}$$

These results can directly be extended to the LL → TT configuration using (B.22).

Mixed polarizations: TL → TL and LT → LT. For the TL → TL configuration, the contribution (B.20) of soft neutral gauge bosons gives

$$\sum_{N=A,Z}\delta^{N,\mathrm{SSC}}_{\mathrm{W}_{\tau_1}^-\mathrm{W}_0^+\to\mathrm{W}_{-\tau_3}^-\mathrm{W}_0^+} = \\ = -\frac{\alpha}{2\pi s_\mathrm{W}^2}\log\left(\frac{|r_{12}|}{M_\mathrm{W}^2}\right)\left[\log\left(\frac{|r_{13}|}{|r_{23}|}\right)+\frac{1}{4c_\mathrm{W}^2}\log\left(\frac{|r_{13}|}{|r_{12}|}\right)\right]-4\log\left(\frac{|r_{13}|}{|r_{23}|}\right)l^{\mathrm{EM}}_{\mathrm{SSC}}. \tag{B.29}$$

JHEP03(2007)078

Soft virtual W bosons (B.21) yield

$$\sum_{V=W^\pm} \delta^{V,\mathrm{SSC}} \mathcal{M}^{W_{\tau_1}^- W_0^+ W_{\tau_3}^+ W_0^-} = \frac{\alpha}{2\pi} \log\left(\frac{|r_{12}|}{M_\mathrm{W}^2}\right) \log\left(\frac{|r_{13}|}{|r_{12}|}\right)$$
$$\times \left[\sum_{N=A,Z} \sum_{N'=A,Z} J_N^- J_{N'}^+ \mathcal{M}_0^{N_{\tau_1} W_0^+ N'_{\tau_3} W_0^-} + \sum_{S=H,Z_0} \sum_{S'=H,Z_0} J_S^+ J_{S'}^- \mathcal{M}_0^{W_{\tau_1}^- S W_{\tau_3}^+ S'} \right]$$
$$= \frac{\alpha}{2\pi} \log\left(\frac{|r_{12}|}{M_\mathrm{W}^2}\right) \log\left(\frac{|r_{13}|}{|r_{12}|}\right) \Bigg\{ -\mathcal{M}_0^{A_{\tau_1} W_0^+ A_{\tau_3} W_0^-} - \frac{c_\mathrm{W}^2}{s_\mathrm{W}^2} \mathcal{M}_0^{Z_{\tau_1} W_0^+ Z_{\tau_3} W_0^-}$$
$$+ \frac{c_\mathrm{W}}{s_\mathrm{W}} \left[\mathcal{M}_0^{A_{\tau_1} W_0^+ Z_{\tau_3} W_0^-} + (A \leftrightarrow Z) \right] + \frac{1}{4 s_\mathrm{W}^2} \Bigg[\left(\mathcal{M}_0^{W_{\tau_1}^- H W_{\tau_3}^+ H} + \mathcal{M}_0^{W_{\tau_1}^- H W_{\tau_3}^+ Z_0} \right)$$
$$- (H \leftrightarrow Z_0) \Bigg] \Bigg\}. \tag{B.30}$$

Using the Born amplitudes (D.16), (D.17) in the high-energy limit we obtain the relative correction

$$\sum_{V=W^\pm} \delta^{V,\mathrm{SSC}}_{\mathrm{W}_{\tau_1}^- \mathrm{W}_0^+ \to \mathrm{W}_{-\tau_3}^- \mathrm{W}_0^+} = -\frac{\alpha}{2\pi s_\mathrm{W}^2} \left(\frac{r_{12}}{r_{23}} + \frac{1}{2} \right) \log\left(\frac{|r_{12}|}{M_\mathrm{W}^2}\right) \log\left(\frac{|r_{13}|}{|r_{12}|}\right). \tag{B.31}$$

These results can directly be extended to the LT → LT configuration using (B.22).

Purely transverse polarizations. The contribution (B.20) of soft neutral gauge bosons gives

$$\sum_{N=A,Z} \delta^{N,\mathrm{SSC}}_{\mathrm{W}_{\tau_1}^- \mathrm{W}_{\tau_2}^+ \to \mathrm{W}_{-\tau_3}^- \mathrm{W}_{-\tau_4}^+} = -\frac{\alpha}{\pi s_\mathrm{W}^2} \log\left(\frac{|r_{12}|}{M_\mathrm{W}^2}\right) \log\left(\frac{|r_{13}|}{|r_{23}|}\right) - 4 \log\left(\frac{|r_{13}|}{|r_{23}|}\right) l_\mathrm{SSC}^\mathrm{EM}. \tag{B.32}$$

Soft virtual W bosons (B.21) yield

$$\sum_{V=W^\pm} \delta^{V,\mathrm{SSC}} \mathcal{M}^{W_{\tau_1}^- W_{\tau_2}^+ W_{\tau_3}^+ W_{\tau_4}^-} =$$
$$= \frac{\alpha}{2\pi} \log\left(\frac{|r_{12}|}{M_\mathrm{W}^2}\right) \log\left(\frac{|r_{13}|}{|r_{12}|}\right) \sum_{N,N'=A,Z} J_N^- J_{N'}^+ \left[\mathcal{M}_0^{N_{\tau_1} W_{\tau_2}^+ N'_{\tau_3} W_{\tau_4}^-} + \mathcal{M}_0^{W_{\tau_1}^- N'_{\tau_2} W_{\tau_3}^+ N_{\tau_4}} \right]$$
$$= \frac{\alpha}{2\pi} \log\left(\frac{|r_{12}|}{M_\mathrm{W}^2}\right) \log\left(\frac{|r_{13}|}{|r_{12}|}\right) \Bigg\{ -\left(\mathcal{M}_0^{A_{\tau_1} W_{\tau_2}^+ A_{\tau_3} W_{\tau_4}^-} + \mathcal{M}_0^{W_{\tau_1}^- A_{\tau_2} W_{\tau_3}^+ A_{\tau_4}} \right)$$
$$+ \frac{c_\mathrm{W}}{s_\mathrm{W}} \left[\left(\mathcal{M}_0^{A_{\tau_1} W_{\tau_2}^+ Z_{\tau_3} W_{\tau_4}^-} + \mathcal{M}_0^{W_{\tau_1}^- A_{\tau_2} W_{\tau_3}^+ Z_{\tau_4}} \right) + (A \leftrightarrow Z) \right]$$
$$- \frac{c_\mathrm{W}^2}{s_\mathrm{W}^2} \left(\mathcal{M}_0^{Z_{\tau_1} W_{\tau_2}^+ Z_{\tau_3} W_{\tau_4}^-} + \mathcal{M}_0^{W_{\tau_1}^- Z_{\tau_2} W_{\tau_3}^+ Z_{\tau_4}} \right) \Bigg\}. \tag{B.33}$$

In the high-energy limit, using (D.25) we obtain the relative correction factor

$$\sum_{V=W^\pm} \delta^{V,\mathrm{SSC}}_{\mathrm{W}_{\tau_1}^- \mathrm{W}_{\tau_2}^+ \to \mathrm{W}_{-\tau_3}^- \mathrm{W}_{-\tau_4}^+} = \frac{\alpha}{\pi s_\mathrm{W}^2} \frac{r_{13}}{r_{23}} \log\left(\frac{|r_{12}|}{M_\mathrm{W}^2}\right) \log\left(\frac{|r_{13}|}{|r_{12}|}\right). \tag{B.34}$$

JHEP03(2007)078

B.4 Single logarithms from collinear singularities

The single-logarithms originating from collinear singularities associated to external transverse or longitudinal W bosons can be obtained from eqs. (4.10) and (4.33) in ref. [12]. Here we have included also the logarithms of $m_{\rm t}/M_{\rm W}$ and $M_{\rm H}/M_{\rm W}$, which can be found in ref. [14]. The resulting corrections to all processes (B.8) can be expressed by the following general formula, which only depends on the numbers $n_{\rm T}, n_{\rm L}$ of transversely and longitudinally polarized W bosons, respectively.

$$\delta^{\rm C}_{{\rm W}^-_{\lambda_1}{\rm W}^+_{\lambda_2}\to{\rm W}^-_{-\lambda_3}{\rm W}^+_{-\lambda_4}} = \sum_{i=1}^{4}\delta^{\rm C}_{W_{\lambda_i}} = n_{\rm T}\delta^{\rm C}_{W_{\rm T}} + n_{\rm L}\delta^{\rm C}_{W_0}, \tag{B.35}$$

where

$$\delta^{\rm C}_{W_{\rm T}} = \frac{\alpha}{4\pi}\left\{\frac{1}{2}b^{\rm ew}_W \log\left(\frac{|r_{12}|}{M^2_{\rm W}}\right) + \frac{1}{24s^2_{\rm w}}\log\left(\frac{M^2_{\rm H}}{M^2_{\rm W}}\right) + \frac{1}{2s^2_{\rm w}}\log\left(\frac{m^2_{\rm t}}{M^2_{\rm W}}\right)\right\} + l^{\rm EM}(M^2_{\rm W}), \tag{B.36}$$

$$\delta^{\rm C}_{W_0} = \frac{\alpha}{4\pi}\left\{2C^{\rm ew}_\Phi \log\left(\frac{|r_{12}|}{M^2_{\rm W}}\right) - \frac{3}{4s^2_{\rm w}}\frac{m^2_{\rm t}}{M^2_{\rm W}}\log\left(\frac{|r_{12}|}{m^2_{\rm t}}\right) + \frac{1}{8s^2_{\rm w}}\log\left(\frac{M^2_{\rm H}}{M^2_{\rm W}}\right)\right\} + l^{\rm EM}(M^2_{\rm W}),$$

the one-loop coefficient of the SU(2) β-function reads $b^{\rm ew}_W = 19/(6s^2_{\rm w})$, and the electromagnetic contributions $l^{\rm EM}(M^2_{\rm W})$ are defined in (E.3).

B.5 Single logarithms from parameter renormalization

Purely longitudinal polarizations. The renormalization of the parameters $g = e^2/(4s^2_{\rm w}c^2_{\rm w})$ and $\lambda_{\rm H}$ (D.5) in the Born amplitude (D.6) gives rise to the relative correction

$$\delta^{\rm PR}_{{\rm W}^-_0{\rm W}^+_0\to{\rm W}^-_0{\rm W}^+_0} = \frac{\delta g}{g} + \left(\frac{\delta\lambda_{\rm H}}{\lambda_{\rm H}} - \frac{\delta g}{g}\right)\frac{\lambda_{\rm H}}{\lambda_{\rm H} + gA}, \tag{B.37}$$

where

$$A = \frac{r_{13}-r_{23}}{r_{12}} + \frac{r_{12}-r_{23}}{r_{13}} = 2\left(\frac{r^2_{23}}{r_{12}r_{13}} - 1\right) \tag{B.38}$$

in the high-energy limit, and the 't Hooft scale of dimensional regularization has to be set to $\mu^2 = r_{12}$ in the counterterms [12, 13]. In the on-shell scheme (including the tadpole contributions in the renormalization of $\lambda_{\rm H}$) these read [14]

$$\begin{aligned}
\left.\frac{\delta g}{g}\right|_{\mu^2=r_{12}} &= \frac{\alpha}{4\pi}\left\{-b^{\rm ew}_{ZZ}\log\left(\frac{|r_{12}|}{M^2_{\rm W}}\right) + \frac{c^2_{\rm w}-s^2_{\rm w}}{s^2_{\rm w}c^2_{\rm w}}\left[\frac{5}{6}\log\left(\frac{M^2_{\rm H}}{M^2_{\rm W}}\right)\right.\right.\\
&\quad \left.\left. - \frac{9+6s^2_{\rm w}-32s^4_{\rm w}}{18s^2_{\rm w}}\log\left(\frac{m^2_{\rm t}}{M^2_{\rm W}}\right)\right]\right\} + \Delta\alpha(M^2_{\rm W}),\\
\left.\frac{\delta\lambda_{\rm H}}{\lambda_{\rm H}}\right|_{\mu^2=r_{12}} &= \Delta\alpha(M^2_{\rm W}) + \frac{\alpha}{4\pi}\left\{\left\{\frac{3}{2s^2_{\rm w}}\left[\frac{M^2_{\rm W}}{M^2_{\rm H}}\left(2+\frac{1}{c^4_{\rm w}}\right) - \left(2+\frac{1}{c^2_{\rm w}}\right) + \frac{M^2_{\rm H}}{M^2_{\rm W}}\right]\right.\right.\\
&\quad \left.\left. + \frac{N^t_{\rm C}}{s^2_{\rm w}}\frac{m^2_{\rm t}}{M^2_{\rm W}}\left(1-2\frac{m^2_{\rm t}}{M^2_{\rm H}}\right)\right\}\log\left(\frac{|r_{12}|}{M^2_{\rm W}}\right)\right.\\
&\quad + \frac{3}{2s^2_{\rm w}}\left[-\frac{3}{2}\frac{M^2_{\rm W}}{M^2_{\rm H}}\left(2+\frac{1}{c^4_{\rm w}}\right) + \frac{1+2c^2_{\rm w}}{4c^2_{\rm w}} + \frac{10}{9} - \frac{M^2_{\rm H}}{M^2_{\rm W}}\right]\log\left(\frac{M^2_{\rm H}}{M^2_{\rm W}}\right)\\
&\quad \left. - \left[\frac{N^t_{\rm C}}{s^2_{\rm w}}\frac{m^2_{\rm t}}{M^2_{\rm W}}\left(1-2\frac{m^2_{\rm t}}{M^2_{\rm H}}\right) + \frac{9-12s^2_{\rm w}-32s^4_{\rm w}}{18s^4_{\rm w}}\right]\log\left(\frac{m^2_{\rm t}}{M^2_{\rm W}}\right)\right\},
\end{aligned} \tag{B.39}$$

JHEP03(2007)078

where $b^{\rm ew}_{ZZ} = s^2_{\rm W} b^{\rm ew}_B + c^2_{\rm W} b^{\rm ew}_W = (19 - 38 s^2_{\rm W} - 22 s^4_{\rm W})/(6 s^2_{\rm W} c^2_{\rm W})$, with the U(1) and SU(2) one-loop β-function coefficients $b^{\rm ew}_B$ and $b^{\rm ew}_W$ defined in ref. [12], and $\Delta\alpha(M^2_{\rm W})$ represents the running of the electromagnetic coupling constant from the scale 0 to $M_{\rm W}$. Within the G_μ scheme, these effects of the running are already included in the definition of α_{G_μ}. Thus, the $\Delta\alpha(M^2_{\rm W})$-terms appearing in (B.39)–(B.41) were not included in our implementation.

Mixed polarizations. In this case, the Born matrix element is proportional to the squared SU(2) coupling $g_2^2 = e^2/s^2_{\rm W}$. As a result, the parameter renormalization yields

$$\begin{aligned}\delta^{\rm PR}_{{\rm W}^-_{\tau_1}{\rm W}^+_{\tau_2}\to{\rm W}^-_0{\rm W}^+_0} &= \delta^{\rm PR}_{{\rm W}^-_0{\rm W}^+_0\to{\rm W}^-_{-\tau_3}{\rm W}^+_{-\tau_4}} = \delta^{\rm PR}_{{\rm W}^-_{\tau_1}{\rm W}^+_0\to{\rm W}^-_{-\tau_3}{\rm W}^+_0} = \delta^{\rm PR}_{{\rm W}^-_0{\rm W}^+_{\tau_2}\to{\rm W}^-_0{\rm W}^+_{-\tau_4}} = \\ &= 2\frac{\delta g_2}{g_2}\bigg|_{\mu^2=r_{12}} = \frac{\alpha}{4\pi}\left[-b^{\rm ew}_W \log\left(\frac{|r_{12}|}{M^2_{\rm W}}\right) + \frac{5}{6s^2_{\rm W}}\log\left(\frac{M^2_{\rm H}}{M^2_{\rm W}}\right)\right. \\ &\quad \left. - \frac{9 + 6s^2_{\rm W} - 32 s^4_{\rm W}}{18 s^4_{\rm W}}\log\left(\frac{m^2_{\rm t}}{M^2_{\rm W}}\right)\right] + \Delta\alpha(M^2_{\rm W}), \end{aligned} \tag{B.40}$$

with $b^{\rm ew}_W = 19/(6s^2_{\rm W})$. Note that the contribution $b^{\rm ew}_W \log(|r_{12}|/M^2_{\rm W})$ from parameter renormalization cancels a corresponding contribution $b^{\rm ew}_W \log(|r_{12}|/M^2_{\rm W})$ in (B.35), which is associated to the two transverse gauge bosons ($n_{\rm T} = 2$). This cancellation is analogous to the one observed in eq. (A.11) in ref. [12].

Purely transverse polarizations. Also in this case, the Born matrix element is proportional to the squared SU(2) coupling g_2^2 and we have

$$\begin{aligned}\delta^{\rm PR}_{{\rm W}^-_{\tau_1}{\rm W}^+_{\tau_2}\to{\rm W}^-_{-\tau_3}{\rm W}^+_{-\tau_4}} &= \frac{\alpha}{4\pi}\left[-b^{\rm ew}_W \log\left(\frac{|r_{12}|}{M^2_{\rm W}}\right) + \frac{5}{6s^2_{\rm W}}\log\left(\frac{M^2_{\rm H}}{M^2_{\rm W}}\right)\right. \\ &\quad \left. - \frac{9 + 6s^2_{\rm W} - 32 s^4_{\rm W}}{18 s^4_{\rm W}}\log\left(\frac{m^2_{\rm t}}{M^2_{\rm W}}\right)\right] + \Delta\alpha(M^2_{\rm W}). \end{aligned} \tag{B.41}$$

In this case the contributions $b^{\rm ew}_W \log(|r_{12}|/M^2_{\rm W})$ from parameter renormalization cancel only two of the four ($n_{\rm T} = 4$) contributions $b^{\rm ew}_W \log(|r_{12}|/M^2_{\rm W})$ in (B.35).

C. Longitudinal gauge bosons

In order to apply the general formulas of ref. [12] to matrix elements involving longitudinal gauge bosons $V^a_0 = W^\pm_0, Z_0$, these have to be transformed first into corresponding matrix elements involving would-be Goldstone bosons $\Phi_a = \phi^\pm, \chi$ by means of the Goldstone-Boson Equivalence Theorem (GBET) in its naive lowest-order form,[3]

$$\mathcal{M}^{\varphi_{i_1}\dots V^a_0\dots\varphi_{i_n}} = {\rm i}^{1-Q_{V^a}}\mathcal{M}^{\varphi_{i_1}\dots\Phi_a\dots\varphi_{i_n}}, \tag{C.1}$$

where $\varphi_{i_1},\dots\varphi_{i_n}$ represent arbitrary particles with arbitrary polarizations and Q_{V^a} is the gauge-boson charge, i.e. $Q_{W^\pm} = \pm 1$ and $Q_Z = 0$.

[3]The relevant quantum corrections to the GBET, which contribute to the collinear single-logarithms are already taken into account into the corresponding corrections factors (4.33) in ref. [12].

JHEP03(2007)078

Particular care must be taken of the angular-dependent subleading soft-collinear corrections (see eqs. (3.9)–(3.12) of ref. [12])

$$\delta^{\mathrm{SSC}}\mathcal{M}^{\varphi_{i_1}\cdots\varphi_{i_n}} = \\ = \frac{\alpha}{2\pi}\sum_{k=1}^{n}\sum_{l<k}\sum_{V^a=A,Z,W^\pm}\log\left(\frac{|r_{12}|}{M_a^2}\right)\log\left(\frac{|r_{kl}|}{|r_{12}|}\right)I^{V^a}_{\varphi_{i_l'}\varphi_{i_l}}I^{\bar{V}^a}_{\varphi_{i_k'}\varphi_{i_k}}\mathcal{M}_0^{\varphi_{i_1}\cdots\varphi_{i_l'}\cdots\varphi_{i_k'}\cdots\varphi_{i_n}}, \quad \text{(C.2)}$$

which involve non-abelian couplings $I^{V^a}_{\varphi_{i'}\varphi_i}$ that are in general non-diagonal and lead therefore to SU(2)-transformed Born matrix elements with $\varphi_{i'} \neq \varphi_i$ on the right-hand side of (C.2). For processes involving longitudinal gauge bosons and Higgs bosons, this formula has to be applied to corresponding processes involving would-be Goldstone bosons and Higgs bosons. Then the unphysical matrix elements on the left- and right-hand sides of (C.2) have to be transformed into physical matrix elements by means of the GBET. In doing this, the factors $\mathrm{i}^{1-Q_{V^a}}$ originating from the GBET (C.1) must be carefully taken into account, since the would-be Goldstone bosons and Higgs bosons appearing on the left- and right-hand side of (C.2) (and thus the corresponding GBET factors) can be different.

In order to avoid these complications related to the explicit use of the GBET, in the following we introduce effective couplings for longitudinal gauge bosons and Higgs bosons, which permit to apply (C.2) directly to physical matrix elements. To this end the factors $\mathrm{i}^{1-Q_{V^a}}$ from the GBET are combined with the gauge couplings for would-be Goldstone bosons and Higgs bosons, resulting into the effective couplings

$$I^{V^c}_{V_0^bV_0^a} = (-\mathrm{i})^{1-Q_{V^b}}I^{V^c}_{\Phi_b\Phi_a}\mathrm{i}^{1-Q_{V^a}}, \qquad I^{V^c}_{HV_0^a} = I^{V^c}_{H\Phi_a}\mathrm{i}^{1-Q_{V^a}}, \qquad I^{V^c}_{V_0^bH} = (-\mathrm{i})^{1-Q_{V^b}}I^{V^c}_{\Phi_bH}, \quad \text{(C.3)}$$

where $V^c = A, Z, W^\pm$, and $\Phi_a = \phi^\pm, \chi$ are the would-be Goldstone bosons corresponding to $V_0^a = W_0^\pm, Z_0$. We observe that the relations (C.1) and (C.3) can be regarded as the result of a reparametrization of the scalar sector through the the unitary transformation

$$\Phi_a = \mathrm{i}^{1-Q_{V^a}}V_0^a. \quad \text{(C.4)}$$

If one performs this transformation directly at the level of the Lagrangian one can express the Feynman rules in terms of the longitudinal gauge-boson fields. This simplifies the calculation of matrix elements for longitudinal gauge bosons in the high-energy limit (see appendix D). The Feynman rules for the scalar and gauge interactions of the fields $S_i = W_0^\pm, Z_0, H$ and their propagators in the 't Hooft-Feynman gauge read

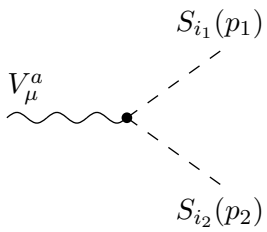

$$= \mathrm{i}eI^{V^{a_1}}_{S_{i_1}^+S_{i_2}}(p_2-p_1)_{\mu_1}, \quad \text{(C.5)}$$

JHEP03(2007)078

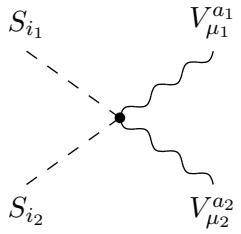

$$= \mathrm{i}e^2 g_{\mu_1\mu_2} \left\{ I^{V^{a_1}}, I^{V^{a_2}} \right\}_{S_{i_1}^+ S_{i_2}}, \tag{C.6}$$

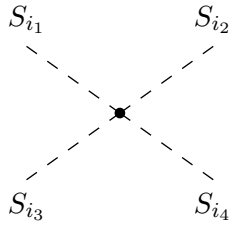

$$= -\mathrm{i}\frac{\lambda_\mathrm{H}}{2} \left[\delta_{S_{i_1}^+ S_{i_2}} \delta_{S_{i_3}^+ S_{i_4}} + (2 \leftrightarrow 3) + (2 \leftrightarrow 4) \right], \tag{C.7}$$

$$= \frac{\mathrm{i}\,\delta_{S_i^+ S_j}}{p^2 - M_{S_i}^2}. \tag{C.8}$$

Here, all fields are incoming, the curly brackets represent an anticommutator and products of couplings have to be understood as

$$\left(I^{V^{a_1}} I^{V^{a_2}} \right)_{S_i S_j} = \sum_{S_k = W_0^\pm, Z_0, H} I^{V^{a_1}}_{S_i S_k} I^{V^{a_2}}_{S_k S_j}. \tag{C.9}$$

The Feynman rules (C.5)–(C.8) are closely analogous to those in ref. [14]. However here, as a result of the unitary transformation (C.4), the hermitian conjugation of the fields $V_0^a = Z_0, W_0^\pm$ generates a minus sign,

$$V_0^{a+} = -\bar{V}_0^a, \tag{C.10}$$

where $\bar{V}_0^a = (-\mathrm{i})^{(1-Q_{\bar{V}^a})} \Phi_a^+$ or, equivalently, $\bar{W}_0^\pm = W_0^\mp$ and $\bar{Z}_0 = Z_0$. As a consequence, the coupling matrices and the Kronecker symbols that involve hermitian conjugate fields in (C.5)–(C.8) have to be understood as

$$I^{V^a}_{S_i^+ S_j} = -I^{V^a}_{\bar{S}_i S_j}, \qquad \delta_{S_i^+ S_j} = -\delta_{\bar{S}_i S_j} \tag{C.11}$$

for $S_i = W_0^\pm, Z_0$. Instead, $H^+ = \bar{H} = H$ for the Higgs field, and

$$I^{V^a}_{H^+ S_j} = I^{V^a}_{H S_j}, \qquad \delta_{H^+ S_j} = \delta_{H S_j}. \tag{C.12}$$

Below we list the explicit expression for all non-vanishing effective couplings (C.3), which can be easily derived from eqs. (B.21)–(B-23) in ref. [12]. For neutral gauge bosons ($N = A, Z$) we have

$$I^N_{W_0^\sigma W_0^{\sigma'}} = \delta_{\sigma\sigma'} I^N_{W_0^\sigma}, \qquad \text{with} \qquad I^A_{W_0^\sigma} = -\sigma, \qquad I^Z_{W^\sigma} = \sigma \frac{1 - 2s_\mathrm{W}^2}{2 s_\mathrm{W} c_\mathrm{W}}, \tag{C.13}$$

JHEP03(2007)078

and

$$I^N_{Z_0H} = I^N_{HZ_0} = \delta_{NZ}\frac{1}{2s_{\mathrm{W}}c_{\mathrm{W}}}. \tag{C.14}$$

For charged gauge bosons coupling to $S = Z_0, H$ we obtain,

$$I^{W^{\sigma'}}_{W_0^\sigma S} = I^{W^{-\sigma'}}_{SW_0^\sigma} = -\delta_{\sigma\sigma'}J^\sigma_S, \qquad J^\sigma_{Z_0} = \sigma\frac{1}{2s_{\mathrm{W}}}, \qquad J^\sigma_H = -\frac{1}{2s_{\mathrm{W}}}. \tag{C.15}$$

Note that the couplings (C.15) are analogous to the couplings for transverse gauge bosons defined in (B.26) of ref. [12], which can also be written as

$$I^{W^{\sigma'}}_{W^\sigma_{\mathrm{T}}N_{\mathrm{T}}} = I^{W^{-\sigma'}}_{N_{\mathrm{T}}W^\sigma_{\mathrm{T}}} = -\delta_{\sigma\sigma'}J^\sigma_{N_{\mathrm{T}}}, \qquad J^\sigma_{A_{\mathrm{T}}} = -\sigma, \qquad J^\sigma_{Z_{\mathrm{T}}} = \sigma\frac{c_{\mathrm{W}}}{s_{\mathrm{W}}}. \tag{C.16}$$

D. Born matrix elements in the high-energy limit

As input for the evaluation of the angular-dependent subleading corrections (B.21), which originate from exchange of soft-collinear W bosons, we need the SU(2)-transformed Born matrix elements that appear on the right-hand side of (B.21). The needed amplitudes are evaluated in the following in high-energy approximation, i.e. omitting mass-suppressed terms. For longitudinal gauge bosons or Higgs bosons, which are denoted as

$$S_i = W_0^\pm, Z_0, H, \qquad \bar{S}_i = W_0^\mp, Z_0, H, \tag{D.1}$$

we use the couplings introduced in appendix C. Transverse gauge bosons are denoted as

$$V^a_\tau = A_\tau, Z_\tau, W^\pm_\tau, \qquad \bar{V}^a_\tau = A_\tau, Z_\tau, W^\mp_\tau, \tag{D.2}$$

with $\tau = \pm 1$.

Purely longitudinal polarizations: LL → LL. For a generic process

$$S_{i_1}(k_1)S_{i_2}(k_2) \to \bar{S}_{i_3}(-k_3)\bar{S}_{i_4}(-k_4), \tag{D.3}$$

in the high-energy limit we obtain the amplitude

$$\begin{aligned}\mathcal{M}_0^{S_{i_1}S_{i_2}S_{i_3}S_{i_4}} = &\left(e^2\,\frac{r_{13}-r_{23}}{r_{12}}\sum_{V^a=A,Z,W^\pm} I^{V^a}_{S^+_{i_1}S_{i_2}}I^{\bar{V}^a}_{S^+_{i_3}S_{i_4}} - \frac{\lambda_{\mathrm{H}}}{2}\,\delta_{S^+_{i_1}S_{i_2}}\delta_{S^+_{i_3}S_{i_4}}\right)\\ &+ (2\leftrightarrow 3) + (1\leftrightarrow 3),\end{aligned} \tag{D.4}$$

where

$$\lambda_{\mathrm{H}} = \frac{e^2}{2s^2_{\mathrm{W}}}\frac{M^2_{\mathrm{H}}}{M^2_{\mathrm{W}}}, \tag{D.5}$$

is the scalar self-coupling.

The Born matrix element for W-boson scattering reads

$$\mathcal{M}_0^{W_0^-W_0^+W_0^+W_0^-} = -\left[\lambda_{\mathrm{H}} + \frac{e^2}{4s^2_{\mathrm{W}}c^2_{\mathrm{W}}}\left(\frac{r_{13}-r_{23}}{r_{12}} + \frac{r_{12}-r_{23}}{r_{13}}\right)\right]. \tag{D.6}$$

JHEP03(2007)078

The SU(2)-transformed Born matrix elements involving two equal neutral states, $S = H$ or Z_0, give

$$\mathcal{M}_0^{SW_0^+SW_0^-} = \mathcal{M}_0^{W_0^-SW_0^+S} = \epsilon_S \left[\frac{\lambda_{\rm H}}{2} + \frac{e^2}{4s_{\rm W}^2} \left(\frac{r_{13} - r_{23}}{r_{12}} + \frac{r_{13} - r_{12}}{r_{23}} \right) \right], \tag{D.7}$$

with $\epsilon_H = 1$ and $\epsilon_{Z_0} = -1$. For the case of different neutral states, $S \neq S'$ with $S, S' = H$ or Z_0, we have

$$\begin{aligned} \mathcal{M}_0^{SW_0^+S'W_0^-} &= \mathcal{M}_0^{W_0^-S'W_0^+S} = \\ &= -\epsilon_S e^2 \left[\frac{1}{4s_{\rm W}^2} \left(\frac{r_{13} - r_{23}}{r_{12}} - \frac{r_{13} - r_{12}}{r_{23}} \right) + \frac{s_{\rm W}^2 - c_{\rm W}^2}{4s_{\rm W}^2 c_{\rm W}^2} \frac{r_{12} - r_{23}}{r_{13}} \right]. \end{aligned} \tag{D.8}$$

Mixed polarizations: TT → LL and LL → TT. For a generic TT → LL process,

$$V_{\tau_1}^{a_1}(k_1) V_{\tau_2}^{a_2}(k_2) \to \bar{S}_{i_3}(-k_3) \bar{S}_{i_4}(-k_4), \tag{D.9}$$

in the high-energy limit we obtain the amplitude

$$\mathcal{M}_0^{V_{\tau_1}^{a_1} V_{\tau_2}^{a_2} S_{i_3} S_{i_4}} = 2e^2 (1 - \delta_{\tau_1 \tau_2}) \left[\frac{r_{23}}{r_{12}} \left(I^{V^{a_1}} I^{V^{a_2}} \right)_{S_{i_3}^+ S_{i_4}} + \frac{r_{13}}{r_{12}} \left(I^{V^{a_2}} I^{V^{a_1}} \right)_{S_{i_3}^+ S_{i_4}} \right]. \tag{D.10}$$

Inserting the explicit values of the couplings we obtain

$$\mathcal{M}_0^{W_{\tau_1}^- W_{\tau_2}^+ W_0^+ W_0^-} = -\frac{e^2}{s_{\rm W}^2} (1 - \delta_{\tau_1 \tau_2}) \frac{r_{23}}{r_{12}}, \tag{D.11}$$

and the SU(2)-transformed amplitudes

$$\begin{aligned} \mathcal{M}_0^{N_{\tau_1} W_{\tau_2}^+ H W_0^-} &= -\mathcal{M}_0^{W_{\tau_1}^- N_{\tau_2} W_0^+ H} = -\mathcal{M}_0^{N_{\tau_1} W_{\tau_2}^+ Z_0 W_0^-} = -\mathcal{M}_0^{W_{\tau_1}^- N_{\tau_2} W_0^+ Z_0} \\ &= \frac{e^2}{s_{\rm W}} (1 - \delta_{\tau_1 \tau_2}) \frac{r_{23}}{r_{12}} D_N, \end{aligned} \tag{D.12}$$

with $N_\tau = A_\tau, Z_\tau$, and

$$D_A = \frac{r_{13}}{r_{23}}, \qquad D_Z = \frac{1}{2 s_{\rm W} c_{\rm W}} - \frac{r_{13}}{r_{23}} \frac{1 - 2s_{\rm W}^2}{2 s_{\rm W} c_{\rm W}}. \tag{D.13}$$

Corresponding amplitudes for LL → TT processes are directly obtained using $\mathcal{M}_0^{S_{i_1} S_{i_2} V_{\tau_3}^{a_3} V_{\tau_4}^{a_4}} = \mathcal{M}_0^{V_{\tau_4}^{a_4} V_{\tau_3}^{a_3} S_{i_2} S_{i_1}}$.

Mixed polarizations: TL → TL and LT → LT. For a generic TL → TL process

$$V_{\tau_1}^{a_1}(k_1) S_{i_2}(k_2) \to \bar{V}_{-\tau_3}^{a_3}(-k_3) \bar{S}_{i_4}(-k_4), \tag{D.14}$$

in the high-energy limit we obtain the amplitude

$$\mathcal{M}_0^{V_{\tau_1}^{a_1} S_{i_2} V_{\tau_3}^{a_3} S_{i_4}} = 2e^2 (1 - \delta_{\tau_1 \tau_3}) \left[\frac{r_{23}}{r_{13}} \left(I^{V^{a_1}} I^{V^{a_3}} \right)_{S_{i_2}^+ S_{i_4}} + \frac{r_{12}}{r_{13}} \left(I^{V^{a_3}} I^{V^{a_1}} \right)_{S_{i_2}^+ S_{i_4}} \right]. \tag{D.15}$$

JHEP03(2007)078

Inserting the explicit values of the couplings we obtain the Born amplitude

$$\mathcal{M}_0^{W^-_{\tau_1}W^+_0W^+_{\tau_3}W^-_0} = -\frac{e^2}{s_{\rm W}^2}(1-\delta_{\tau_1\tau_3})\frac{r_{23}}{r_{13}}, \tag{D.16}$$

and the SU(2)-transformed amplitudes

$$\begin{aligned}
\mathcal{M}_0^{N_{\tau_1}W^+_0N'_{\tau_3}W^-_0} &= 2e^2(1-\delta_{\tau_1\tau_3})I^N_{W^+_0}I^{N'}_{W^+_0},\\
\mathcal{M}_0^{W^-_{\tau_1}HW^+_{\tau_3}H} &= -\mathcal{M}_0^{W^-_{\tau_1}Z_0W^+_{\tau_3}Z_0} = -\frac{e^2}{2s_{\rm W}^2}(1-\delta_{\tau_1\tau_3}),\\
\mathcal{M}_0^{W^-_{\tau_1}HW^+_{\tau_3}Z_0} &= -\mathcal{M}_0^{W^-_{\tau_1}Z_0W^+_{\tau_3}H} = \frac{e^2}{2s_{\rm W}^2}(1-\delta_{\tau_1\tau_3})\frac{r_{12}-r_{23}}{r_{13}},
\end{aligned} \tag{D.17}$$

with $N_\tau = A_\tau, Z_\tau$, $I^A_{W^+_0} = -1$ and $I^Z_{W^+_0} = (1-2s_{\rm W}^2)/(2s_{\rm W}c_{\rm W})$.

Corresponding amplitudes for LT $\to$ LT processes are directly obtained using $\mathcal{M}_0^{S_{i_1}V^{a_2}_{\tau_2}S_{i_3}V^{a_4}_{\tau_4}} = \mathcal{M}_0^{V^{a_4}_{\tau_4}S_{i_3}V^{a_2}_{\tau_2}S_{i_1}}$.

Purely transverse polarizations: TT $\to$ TT**.** For a generic process

$$V^{a_1}_{\tau_1}(k_1)V^{a_2}_{\tau_2}(k_2) \to \bar{V}^{a_3}_{-\tau_3}(-k_3)\bar{V}^{a_4}_{-\tau_4}(-k_4), \tag{D.18}$$

in the high-energy limit we obtain the amplitude

$$\begin{aligned}
\mathcal{M}_0^{V^{a_1}_{\tau_1}V^{a_2}_{\tau_2}V^{a_3}_{\tau_3}V^{a_4}_{\tau_4}} = 2\frac{e^2}{s_{\rm W}^2}\Big[&\left(\delta^{\rm SU(2)}_{\bar{V}^{a_1}V^{a_2}}\delta^{\rm SU(2)}_{\bar{V}^{a_3}V^{a_4}} - \delta^{\rm SU(2)}_{\bar{V}^{a_1}V^{a_3}}\delta^{\rm SU(2)}_{\bar{V}^{a_2}V^{a_4}}\right)A(\vec{\tau},\{r_{ij}\})\\
&+\left(\delta^{\rm SU(2)}_{\bar{V}^{a_1}V^{a_2}}\delta^{\rm SU(2)}_{\bar{V}^{a_3}V^{a_4}} - \delta^{\rm SU(2)}_{\bar{V}^{a_1}V^{a_4}}\delta^{\rm SU(2)}_{\bar{V}^{a_3}V^{a_2}}\right)B(\vec{\tau},\{r_{ij}\})\Big],
\end{aligned} \tag{D.19}$$

where the matrix $\delta^{\rm SU(2)}$ is defined in appendix B.2 of ref. [14], and has the non-vanishing components $\delta^{\rm SU(2)}_{AA} = s_{\rm W}^2$, $\delta^{\rm SU(2)}_{ZZ} = c_{\rm W}^2$, $\delta^{\rm SU(2)}_{AZ} = \delta^{\rm SU(2)}_{ZA} = -c_{\rm W}s_{\rm W}$, $\delta^{\rm SU(2)}_{W^+W^+} = \delta^{\rm SU(2)}_{W^-W^-} = 1$. The functions A, B depend on the invariants r_{ij} and the polarizations $\vec{\tau} = (\tau_1,\tau_2,\tau_3,\tau_4)$. The only combinations of polarizations that yield non-vanishing contributions are

$$\vec{\tau}_a = (\sigma,\sigma,-\sigma,-\sigma), \qquad \vec{\tau}_b = (\sigma,-\sigma,\sigma,-\sigma), \qquad \vec{\tau}_c = (-\sigma,\sigma,\sigma,-\sigma) \tag{D.20}$$

with $\sigma = \pm$, and we have

$$A(\vec{\tau}_a,\{r_{ij}\}) = -\frac{r_{12}}{r_{23}}, \qquad A(\vec{\tau}_b,\{r_{ij}\}) = -\frac{r_{13}^2}{r_{12}r_{23}}, \qquad A(\vec{\tau}_c,\{r_{ij}\}) = -\frac{r_{23}}{r_{12}}, \tag{D.21}$$

and

$$B(\vec{\tau}_a,\{r_{ij}\}) = -\frac{r_{12}}{r_{13}}, \qquad B(\vec{\tau}_b,\{r_{ij}\}) = -\frac{r_{13}}{r_{12}}, \qquad B(\vec{\tau}_c,\{r_{ij}\}) = -\frac{r_{23}^2}{r_{12}r_{13}}, \tag{D.22}$$

whereas if $\vec{\tau} \neq \vec{\tau}_a, \vec{\tau}_b, \vec{\tau}_c$ then $A(\vec{\tau},\{r_{ij}\}) = B(\vec{\tau},\{r_{ij}\}) = 0$. Inserting the explicit values of the couplings we obtain

$$\mathcal{M}_0^{W^-_{\tau_1}W^+_{\tau_2}W^+_{\tau_3}W^-_{\tau_4}} = \frac{2e^2}{s_{\rm W}^2}B(\vec{\tau},\{r_{ij}\}), \tag{D.23}$$

JHEP03(2007)078

and the SU(2)-transformed matrix elements

$$\mathcal{M}_0^{N_{\tau_1}W^+_{\tau_2}N'_{\tau_3}W^-_{\tau_4}} = \mathcal{M}_0^{W^-_{\tau_1}N'_{\tau_2}W^+_{\tau_3}N_{\tau_4}} = -\frac{2e^2}{s_{\rm W}^2}\delta^{\rm SU(2)}_{N'N}A(\vec{\tau},\{r_{ij}\}), \tag{D.24}$$

for $N, N' = A, Z$. We note that the ratio between the Born amplitudes (D.24) and (D.23),

$$\frac{\mathcal{M}_0^{N_{\tau_1}W^+_{\tau_2}N'_{\tau_3}W^-_{\tau_4}}}{\mathcal{M}_0^{W^-_{\tau_1}W^+_{\tau_2}W^+_{\tau_3}W^-_{\tau_4}}} = \frac{\mathcal{M}_0^{W^-_{\tau_1}N'_{\tau_2}W^+_{\tau_3}N_{\tau_4}}}{\mathcal{M}_0^{W^-_{\tau_1}W^+_{\tau_2}W^+_{\tau_3}W^-_{\tau_4}}} = -\delta^{\rm SU(2)}_{N'N}\frac{A(\vec{\tau},\{r_{ij}\})}{B(\vec{\tau},\{r_{ij}\})} = -\delta^{\rm SU(2)}_{N'N}\frac{r_{13}}{r_{23}}, \tag{D.25}$$

is independent of the polarizations.

E. Electromagnetic virtual and real contributions

In this appendix we provide simple substitutions that permit to generalize the results of ref. [12] to semi-inclusive $2 \to 2$ processes, by including the soft-photon bremsstrahlung corrections.[4] These substitutions concern the infrared-divergent logarithms $L^{\rm em}(s,\lambda^2,m_k^2)$, $l(M_{\rm W}^2,\lambda^2)$, $l^{\rm em}(m_k^2)$ that appear in eqs. (3.7), (3.8), (3.10), (3.12), (4.6), (4.7), (4.10) and (4.33) of ref. [12] and have to be replaced with the logarithms $L^{\rm EM}(m_k^2)$, $l^{\rm em}_{\rm SSC}$ and $l^{\rm EM}(m_k^2)$, defined in the following.

These results are valid for arbitrary $2 \to 2$ processes in the CM frame, with a soft-photon cut-off ΔE. The contributions from virtual photons (superscript 'em') and real bremsstrahlung (superscript 'brems') as well as their sum (superscript 'EM') are given separately and split into leading-, subleading-soft-collinear and collinear (or soft) parts.

Leading soft-collinear contributions. The terms $L^{\rm em}(s,\lambda^2,m_k^2)$, which are defined in eq. (3.8) of ref. [12] and contribute to eq. (3.7) of ref. [12] have to be substituted by $L^{\rm EM}(m_k^2) = L^{\rm em}(m_k^2) + L^{\rm brems}(m_k^2)$, with

$$\begin{aligned}
L^{\rm em}(m_k^2) &= \frac{\alpha}{4\pi}\left\{2\log\left(\frac{|r_{12}|}{m_k^2}\right)\log\left(\frac{M_{\rm W}^2}{\lambda^2}\right) - \log^2\left(\frac{M_{\rm W}^2}{m_k^2}\right)\right\},\\
L^{\rm brems}(m_k^2) &= \frac{\alpha}{4\pi}\left\{\log\left(\frac{|r_{12}|}{m_k^2}\right)\left[2\log\left(\frac{\lambda^2}{4\Delta E^2}\right) + \log\left(\frac{|r_{12}|}{m_k^2}\right)\right]\right\},\\
L^{\rm EM}(m_k^2) &= \frac{\alpha}{4\pi}\left\{-\log^2\left(\frac{|r_{12}|}{M_{\rm W}^2}\right) + 2\log\left(\frac{|r_{12}|}{4\Delta E^2}\right)\log\left(\frac{|r_{12}|}{m_k^2}\right)\right\}.
\end{aligned} \tag{E.1}$$

Subleading soft-collinear contributions. The terms $l(M_{\rm W}^2,\lambda^2)$ in eqs. (3.10) and (3.12) of ref. [12] have to be substituted by $l^{\rm EM}_{\rm SSC} = l^{\rm em}_{\rm SSC} + l^{\rm brems}_{\rm SSC}$, with

$$l^{\rm em}_{\rm SSC} = \frac{\alpha}{4\pi}\log\left(\frac{M_{\rm W}^2}{\lambda^2}\right), \qquad l^{\rm brems}_{\rm SSC} = \frac{\alpha}{4\pi}\log\left(\frac{\lambda^2}{4\Delta E^2}\right), \qquad l^{\rm EM}_{\rm SSC} = \frac{\alpha}{4\pi}\log\left(\frac{M_{\rm W}^2}{4\Delta E^2}\right). \tag{E.2}$$

[4] The soft bremsstrahlung corrections to squared matrix elements factorize into the squared Born matrix elements times correction factors. These latter have been divided by 2 and combined with the virtual correction factors to (non-squared) matrix elements given in ref. [12].

JHEP03(2007)078

Collinear and soft single logarithms. The terms $l^{\rm em}(m_k^2)$, which are defined in eq. (4.7) of ref. [12] and contribute to eqs. (4.6), (4.10) and (4.33) of ref. [12], have to be substituted by $l^{\rm EM}(m_k^2) = l^{\rm em}(m_k^2) + l^{\rm brems}(m_k^2)$, with

$$\begin{aligned} l^{\rm em}(m_k^2) &= \frac{\alpha}{4\pi}\left[\log\left(\frac{M_{\rm W}^2}{\lambda^2}\right) + \frac{1}{2}\log\left(\frac{M_{\rm W}^2}{m_k^2}\right)\right], \\ l^{\rm brems}(m_k^2) &= \frac{\alpha}{4\pi}\left[\log\left(\frac{\lambda^2}{4\Delta E^2}\right) + \log\left(\frac{|r_{12}|}{m_k^2}\right)\right], \\ l^{\rm EM}(m_k^2) &= \frac{\alpha}{4\pi}\left[\log\left(\frac{|r_{12}|}{4\Delta E^2}\right) + \frac{3}{2}\log\left(\frac{M_{\rm W}^2}{m_k^2}\right)\right]. \end{aligned} \tag{E.3}$$

References

[1] B.W. Lee, C. Quigg and H.B. Thacker, *Weak interactions at very high-energies: the role of the Higgs boson mass*, *Phys. Rev.* **D 16** (1977) 1519;
M. Veltman, *Second threshold in weak interactions*, *Acta Phys. Polon.* **B 8** (1977) 475;
M.S. Chanowitz and M.K. Gaillard, *The TeV physics of strongly interacting W's and Z's*, *Nucl. Phys.* **B 261** (1985) 379.

[2] J. Bagger et al., *The strongly interacting W W system: gold plated modes*, *Phys. Rev.* **D 49** (1994) 1246 [hep-ph/9306256].

[3] J.M. Butterworth, B.E. Cox and J.R. Forshaw, *W W scattering at the LHC*, *Phys. Rev.* **D 65** (2002) 096014 [hep-ph/0201098].

[4] J. Bagger et al., *LHC analysis of the strongly interacting W W system: gold plated modes*, *Phys. Rev.* **D 52** (1995) 3878 [hep-ph/9504426].

[5] V.D. Barger, K. Cheung, T. Han and R.J.N. Phillips, *Probing strongly interacting electroweak dynamics through W^+W^-/ZZ ratios at future e^+e^- colliders*, *Phys. Rev.* **D 52** (1995) 3815 [hep-ph/9501379].

[6] M. Golden, T. Han and G. Valencia, *Strongly-interacting electroweak sector: model independent approaches*, hep-ph/9511206.

[7] E. Boos et al., *Strongly interacting vector bosons at TeV e^+e^- linear colliders*, *Phys. Rev.* **D 57** (1998) 1553 [hep-ph/9708310], *Addendum Phys. Rev.* **D 61** (2000) 077901 [hep-ph/9908409].

[8] E. Accomando, A. Ballestrero, S. Bolognesi, E. Maina and C. Mariotti, *Boson-boson scattering and Higgs production at the LHC from a six fermion point of view: four jets $+l\nu$ processes at $\mathcal{O}(\alpha_{em}^6)$*, *JHEP* **03** (2006) 093 [hep-ph/0512219];
E. Accomando, A. Ballestrero, A. Belhouari and E. Maina, *Boson fusion and Higgs production at the LHC in six fermion final states with one charged lepton pair*, hep-ph/0603167.

[9] ECFA/DESY LC Physics Working Group collaboration, J.A. Aguilar-Saavedra et al., *TESLA technical design report part III: physics at an e^+e^- linear collider*, hep-ph/0106315;
American Linear Collider Working Group collaboration, T. Abe et al., *Linear collider physics resource book for Snowmass 2001*, in *Proc. of the APS/DPF/DPB summer study on the future of particle physics (Snowmass 2001)* ed. R. Davidson and C. Quigg,

JHEP03(2007)078

SLAC-R-570, *Resource book for Snowmass 2001*, [hep-ex/0106055, hep-ex/0106056, hep-ex/0106057, hep-ex/0106058];
ACFA Linear Collider Working Group collaboration, K. Abe et al., *Particle physics experiments at JLC*, hep-ph/0109166;*Report from the International Linear Collider Technical Review Committee*, G.A. Loew (SLAC), SLAC-PUB-10024, Jul 2003; R.D. Heuer, *The International Linear Collider ILC: a status report*, *Nucl. Phys.* **154** *(Proc. Suppl.)* (2006) 131.

[10] CLIC Physics Working Group collaboration, E. Accomando et al., *Physics at the CLIC multi-TeV linear collider*, hep-ph/0412251.

[11] M. Kuroda, G. Moultaka and D. Schildknecht, *Direct one loop renormalization of* $SU(2)_L \times U(1)_Y$ *four fermion processes and running coupling constants*, *Nucl. Phys.* **B 350** (1991) 25;
G. Degrassi and A. Sirlin, *Gauge invariant selfenergies and vertex parts of the Standard Model in the pinch technique framework*, *Phys. Rev.* **D 46** (1992) 3104;
W. Beenakker, A. Denner, S. Dittmaier, R. Mertig and T. Sack, *High-energy approximation for on-shell W pair production*, *Nucl. Phys.* **B 410** (1993) 245; *On shell W pair production in the TeV range*, *Phys. Lett.* **B 317** (1993) 622;
A. Denner, S. Dittmaier and R. Schuster, *Radiative corrections to* $\gamma\gamma \to W^+W^-$ *in the electroweak Standard Model*, *Nucl. Phys.* **B 452** (1995) 80 [hep-ph/9503442];
A. Denner, S. Dittmaier and T. Hahn, *Radiative corrections to* $Z\,Z \to Z\,Z$ *in the electroweak Standard Model*, *Phys. Rev.* **D 56** (1997) 117 [hep-ph/9612390];
A. Denner and T. Hahn, *Radiative corrections to* $W^+W^- \to W^+W^-$ *in the electroweak standard model*, *Nucl. Phys.* **B 525** (1998) 27 [hep-ph/9711302];
M. Beccaria, G. Montagna, F. Piccinini, F.M. Renard and C. Verzegnassi, *Rising bosonic electroweak virtual effects at high energy* e^+e^- *colliders*, *Phys. Rev.* **D 58** (1998) 093014 [hep-ph/9805250];
P. Ciafaloni and D. Comelli, *Sudakov enhancement of electroweak corrections*, *Phys. Lett.* **B 446** (1999) 278 [hep-ph/9809321].

[12] A. Denner and S. Pozzorini, *One-loop leading logarithms in electroweak radiative corrections. I: results*, *Eur. Phys. J.* **C 18** (2001) 461 [hep-ph/0010201].

[13] A. Denner and S. Pozzorini, *One-loop leading logarithms in electroweak radiative corrections. II: factorization of collinear singularities*, *Eur. Phys. J.* **C 21** (2001) 63 [hep-ph/0104127].

[14] S. Pozzorini, *Electroweak radiative corrections at high energies*, *doctoral thesis, Universität Zürich, 2001*, hep-ph/0201077.

[15] V.S. Fadin, L.N. Lipatov, A.D. Martin and M. Melles, *Resummation of double logarithms in electroweak high energy processes*, *Phys. Rev.* **D 61** (2000) 094002 [hep-ph/9910338];
J.H. Kühn, A.A. Penin and V.A. Smirnov, *Summing up subleading Sudakov logarithms*, *Eur. Phys. J.* **C 17** (2000) 97 [hep-ph/9912503];
M. Ciafaloni, P. Ciafaloni and D. Comelli, *Bloch-Nordsieck violating electroweak corrections to inclusive TeV scale hard processes*, *Phys. Rev. Lett.* **84** (2000) 4810 [hep-ph/0001142];
M. Melles, *Subleading Sudakov logarithms in electroweak high energy processes to all orders*, *Phys. Rev.* **D 63** (2001) 034003 [hep-ph/0004056];
W. Beenakker and A. Werthenbach, *Electroweak two-loop Sudakov logarithms for on-shell fermions and bosons*, *Nucl. Phys.* **B 630** (2002) 3 [hep-ph/0112030];
A. Denner, M. Melles and S. Pozzorini, *Two-loop electroweak angular-dependent logarithms at high energies*, *Nucl. Phys.* **B 662** (2003) 299 [hep-ph/0301241].

JHEP03(2007)078

[16] A. Denner, B. Jantzen and S. Pozzorini, *Two-loop electroweak next-to-leading logarithmic corrections to massless fermionic processes*, *Nucl. Phys.* **B 761** (2007) 1 [hep-ph/0608326].

[17] M. Beccaria, P. Ciafaloni, D. Comelli, F.M. Renard and C. Verzegnassi, *Logarithmic expansion of electroweak corrections to four-fermion processes in the TeV region*, *Phys. Rev.* **D 61** (2000) 073005 [hep-ph/9906319]; *The role of the top mass in b production at future lepton colliders*, *Phys. Rev.* **D 61** (2000) 011301 [hep-ph/9907389];
M. Beccaria, F.M. Renard and C. Verzegnassi, *Top quark production at future lepton colliders in the asymptotic regime*, *Phys. Rev.* **D 63** (2001) 053013 [hep-ph/0010205]; *The role of universal and non universal Sudakov logarithms in four fermion processes at TeV energies: the one-loop approximation revisited*, *Phys. Rev.* **D 64** (2001) 073008 [hep-ph/0103335]; *Reliability of a high energy one-loop expansion of $e^+e^- \to W^+W^-$ in the SM and in the MSSM*, *Nucl. Phys.* **B 663** (2003) 394 [hep-ph/0304175].

[18] J. Layssac and F.M. Renard, *High energy behaviour of $\gamma\gamma \to f\bar{f}$ processes in SM and MSSM*, *Phys. Rev.* **D 64** (2001) 053018 [hep-ph/0104205];
G.J. Gounaris, J. Layssac and F.M. Renard, *The processes $e^+e^- \to \gamma\gamma$, $Z\gamma$, ZZ in SM and MSSM*, *Phys. Rev.* **D 67** (2003) 013012 [hep-ph/0211327].

[19] S. Dittmaier and M. Kramer, *Electroweak radiative corrections to W-boson production at hadron colliders*, *Phys. Rev.* **D 65** (2002) 073007 [hep-ph/0109062].

[20] E. Accomando, A. Denner and S. Pozzorini, *Electroweak-correction effects in gauge boson pair production at the LHC*, *Phys. Rev.* **D 65** (2002) 073003 [hep-ph/0110114];
W. Hollik and C. Meier, *Electroweak corrections to γ Z production at hadron colliders*, *Phys. Lett.* **B 590** (2004) 69 [hep-ph/0402281];
E. Accomando, A. Denner and C. Meier, *Electroweak corrections to $W\gamma$ and $Z\gamma$ production at the LHC*, *Eur. Phys. J.* **C 47** (2006) 125 [hep-ph/0509234];
E. Accomando and A. Kaiser, *Electroweak corrections and anomalous triple gauge-boson couplings in W W and W Z production at the LHC*, *Phys. Rev.* **D 73** (2006) 093006 [hep-ph/0511088].

[21] E. Accomando, A. Denner and A. Kaiser, *Logarithmic electroweak corrections to gauge-boson pair production at the LHC*, *Nucl. Phys.* **B 706** (2005) 325 [hep-ph/0409247].

[22] E. Maina, S. Moretti, M.R. Nolten and D.A. Ross, *One-loop weak corrections to the $b\bar{b}$ cross section at TeV energy hadron colliders*, *Phys. Lett.* **B 570** (2003) 205 [hep-ph/0307021];
E. Maina, S. Moretti and D.A. Ross, *One-loop weak corrections to γ/Z hadro-production at finite transverse momentum*, *Phys. Lett.* **B 593** (2004) 143 [hep-ph/0403050]; *Weak corrections to gluon-induced top-antitop hadro-production*, *Phys. Lett.* **B 639** (2006) 513 [hep-ph/0603083];
S. Moretti, M.R. Nolten and D.A. Ross, *Weak corrections to four-parton processes*, *Nucl. Phys.* **B 759** (2006) 50 [hep-ph/0606201].

[23] U. Baur and D. Wackeroth, *Electroweak radiative corrections to $p\bar{p} \to W^\pm \to \ell^\pm\nu$ beyond the pole approximation*, *Phys. Rev.* **D 70** (2004) 073015 [hep-ph/0405191].

[24] J.H. Kühn, A. Kulesza, S. Pozzorini and M. Schulze, *Logarithmic electroweak corrections to hadronic $Z + 1$ jet production at large transverse momentum*, *Phys. Lett.* **B 609** (2005) 277 [hep-ph/0408308]; *One-loop weak corrections to hadronic production of Z bosons at large transverse momenta*, *Nucl. Phys.* **B 727** (2005) 368 [hep-ph/0507178];
Electroweak corrections to hadronic photon production at large transverse momenta, *JHEP* **03** (2006) 059 [hep-ph/0508253].

JHEP03(2007)078

[25] J.H. Kühn, A. Scharf and P. Uwer, *Electroweak effects in top-quark pair production at hadron colliders*, hep-ph/0610335.

[26] W. Bernreuther, M. Fücker and Z.-G. Si, *Weak interaction corrections to hadronic top quark pair production*, *Phys. Rev.* **D 74** (2006) 113005 [hep-ph/0610334].

[27] P. Krstonosic, K. Mönig, M. Beyer, E. Schmidt and H. Schröder, *Experimental studies of strong electroweak symmetry breaking in gauge boson scattering and three gauge boson production*, hep-ph/0508179.

[28] W. Kilian and P.M. Zerwas, *ILC: physics scenarios*, *ECONF* **C0508141** (2005) PLEN0003 [hep-ph/0601217].

[29] I. Kuss and H. Spiesberger, *Luminosities for vector boson-vector boson scattering at high-energy colliders*, *Phys. Rev.* **D 53** (1996) 6078 [hep-ph/9507204].

[30] Particle Data Group, W.M. Yao et al., *Review of particle physics*, *J. Phys. G* **33** (2006) 1.

[31] W. Beenakker, F.A. Berends and A.P. Chapovsky, *Radiative corrections to pair production of unstable particles: results for $e^+e^- \to$ 4fermions*, *Nucl. Phys.* **B 548** (1999) 3 [hep-ph/9811481].

[32] A. Denner, S. Dittmaier, M. Roth and D. Wackeroth, *Electroweak radiative corrections to $e^+e^- \to W\,W \to$ 4fermions in double-pole approximation: the RACOONWW approach*, *Nucl. Phys.* **B 587** (2000) 67 [hep-ph/0006307]; *RACOONWW 1.3: a Monte Carlo program for four-fermion production at e^+e^- colliders*, *Comput. Phys. Commun.* **153** (2003) 462 [hep-ph/0209330].

[33] S. Jadach, W. Placzek, M. Skrzypek, B.F.L. Ward and Z. Was, *Final state radiative effects for the exact $O(\alpha)$ YFS exponentiated (un)stable W^+W^- production at and beyond LEP2 energies*, *Phys. Rev.* **D 61** (2000) 113010 [hep-ph/9907436];*Precision predictions for (un)stable W^+W^- pair production at and beyond LEP2 energies*, *Phys. Rev.* **D 65** (2002) 093010 [hep-ph/0007012].

[34] A. Ballestrero, *PHACT: helicity amplitudes for present and future colliders*, hep-ph/9911318.

[35] A. Ballestrero and E. Maina, *A new method for helicity calculations*, *Phys. Lett.* **B 350** (1995) 225 [hep-ph/9403244].

[36] W. Beenakker, A.P. Chapovsky and F.A. Berends, *Non-factorizable corrections to W pair production*, *Phys. Lett.* **B 411** (1997) 203 [hep-ph/9706339]; *Non-factorizable corrections to W-pair production: methods and analytic results*, *Nucl. Phys.* **B 508** (1997) 17 [hep-ph/9707326].

[37] A. Denner, S. Dittmaier and M. Roth, *Non-factorizable photonic corrections to $e^+e^- \to W\,W \to$ 4fermions*, *Nucl. Phys.* **B 519** (1998) 39 [hep-ph/9710521]; *Further numerical results on non-factorizable corrections to $e^+e^- \to$ 4fermions*, *Phys. Lett.* **B 429** (1998) 145 [hep-ph/9803306].

[38] A. Denner and T. Hahn, *Radiative corrections to $W^+W^- \to W^+W^-$ in the electroweak Standard Model*, *Nucl. Phys.* **B 525** (1998) 27 [hep-ph/9711302].

JHEP03(2007)078